Forearc migration in Cascadia and its neotectonic significance

Wells et al 1998

Geology pp 659-652.

"The Big Picture"

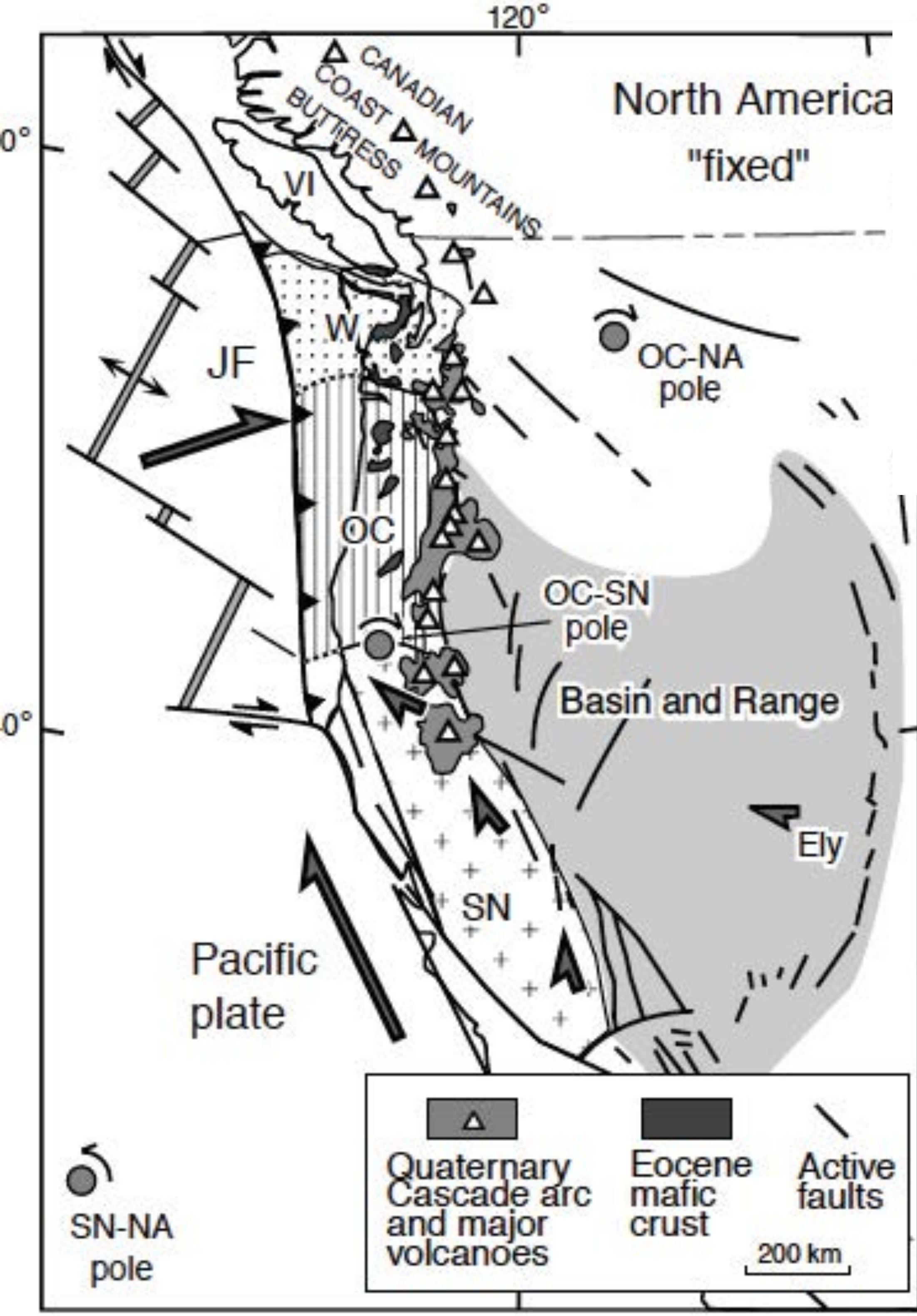

Figure 1. Tectonic setting of Cascadia. Juan de Fuca plate (JF) is subducting (barbed fault) beneath North America. Migrating Cascadia fore-arc terrane divided into Washington (W), Oregon Coastal (OC), and Sierra Nevada blocks (SN). "Instantaneous" Euler rotation poles shown for SN relative to North America (NA), OC-SN, and OC-NA. VI—Vancouver Island. (Modified from Argus and Gordon, 1991; Pezzopane and Weldon, 1993; Walcott, 1993.)

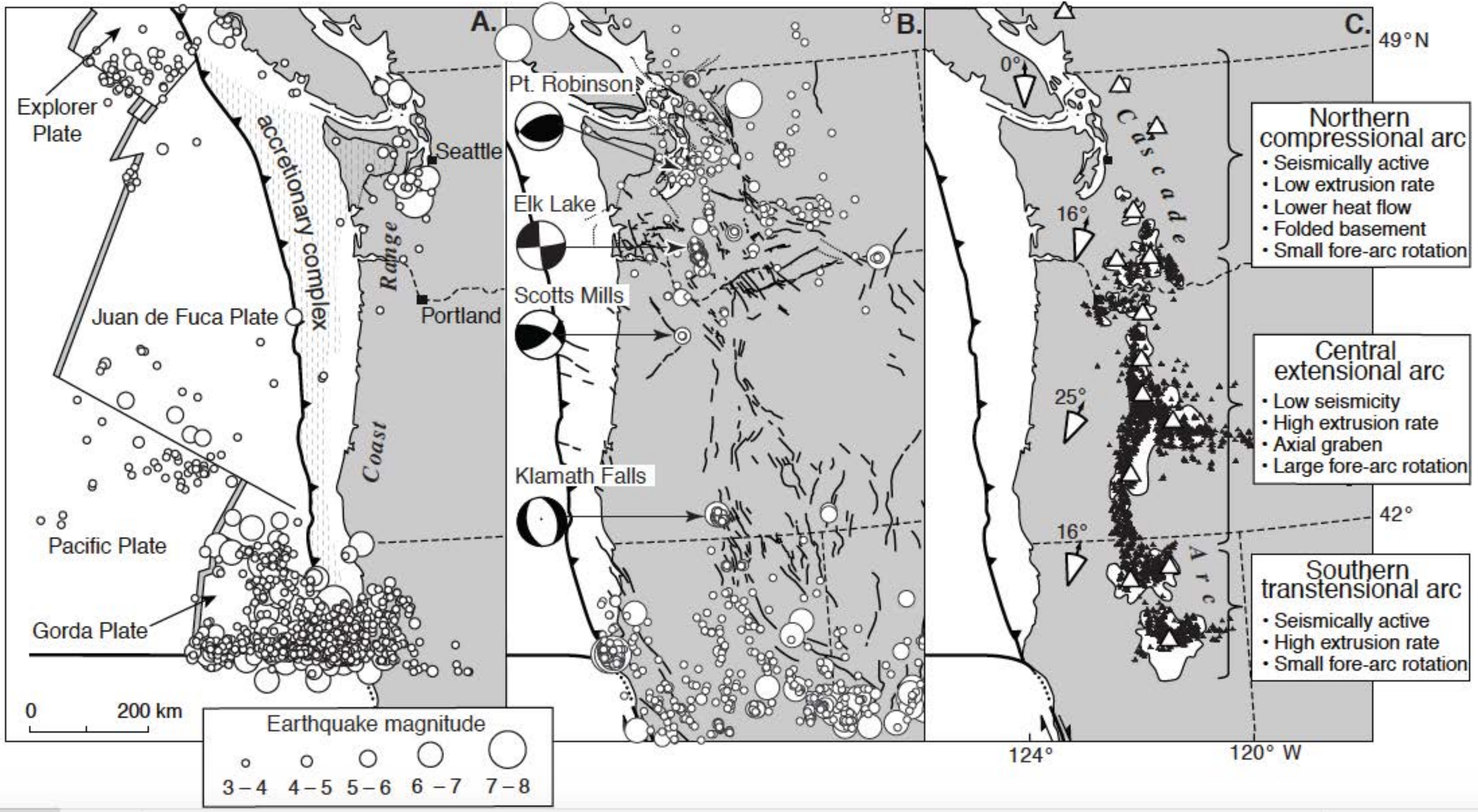

Figure 2. Cascadia earthquakes, faults, volcanoes, and fore-arc rotation (see text). A: Lower plate seismicity. B: Upper plate seismicity, recent focal mechanisms ($M_w > 5$), and late Cenozoic faults. C: Quaternary arc volcanism—white; major volcanoes—open triangles; post–5 Ma volcanic vents—filled triangles; fore-arc rotations with uncertainties—arrows (Pezzopane and Weldon, 1993; Sherrod and Smith, 1990; Guffanti and Weaver, 1988; Wells, 1990; Wiley et al., 1993; Madin et al., 1993).

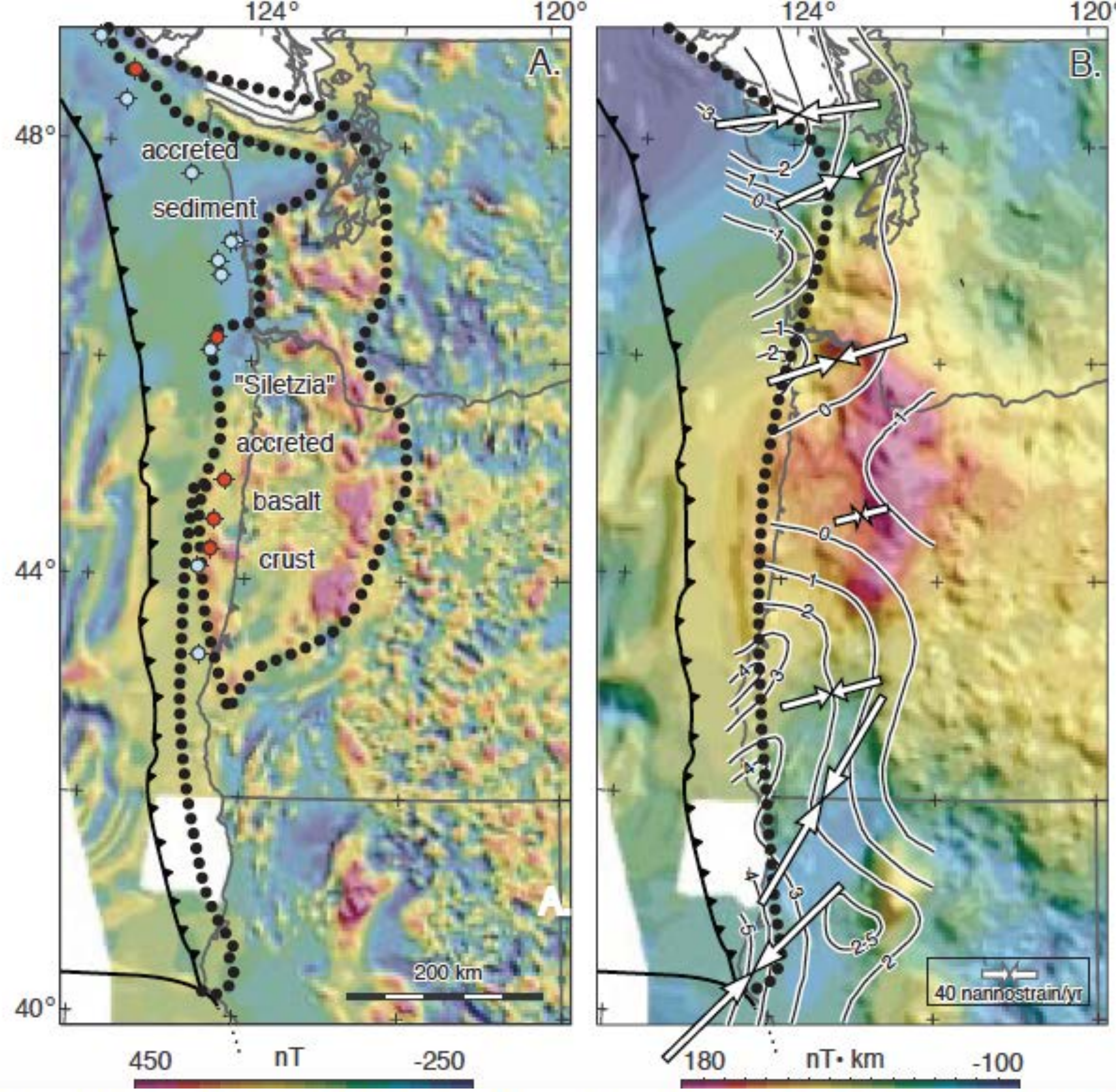

Figure 3. Magnetic and pseudogravity anomalies in the Cascadia fore arc. A: Siletzia, accreted basalt basement shown by magnetic high and offshore wells (filled circles) bottoming in basalt basement (red) and sediment (blue). Accreted sediments (magnetic low) outboard of Siletzia extend south to Mendocino triple junction. B: Pseudogravity anomaly (gravity that would be observed if magnetization were replaced by mass in 1:1 proportion) reflects total volume of Siletzia and coincides with low current uplift and margin contraction (contours in mm/yr, Mitchell et al., 1994; Murray and Lisowski, 1994, and 1998, written commun.) representing elastic strain accumulation above the locked subduction zone. Eastward limit of coupling (dotted) from Hyndman and Wang (1995).

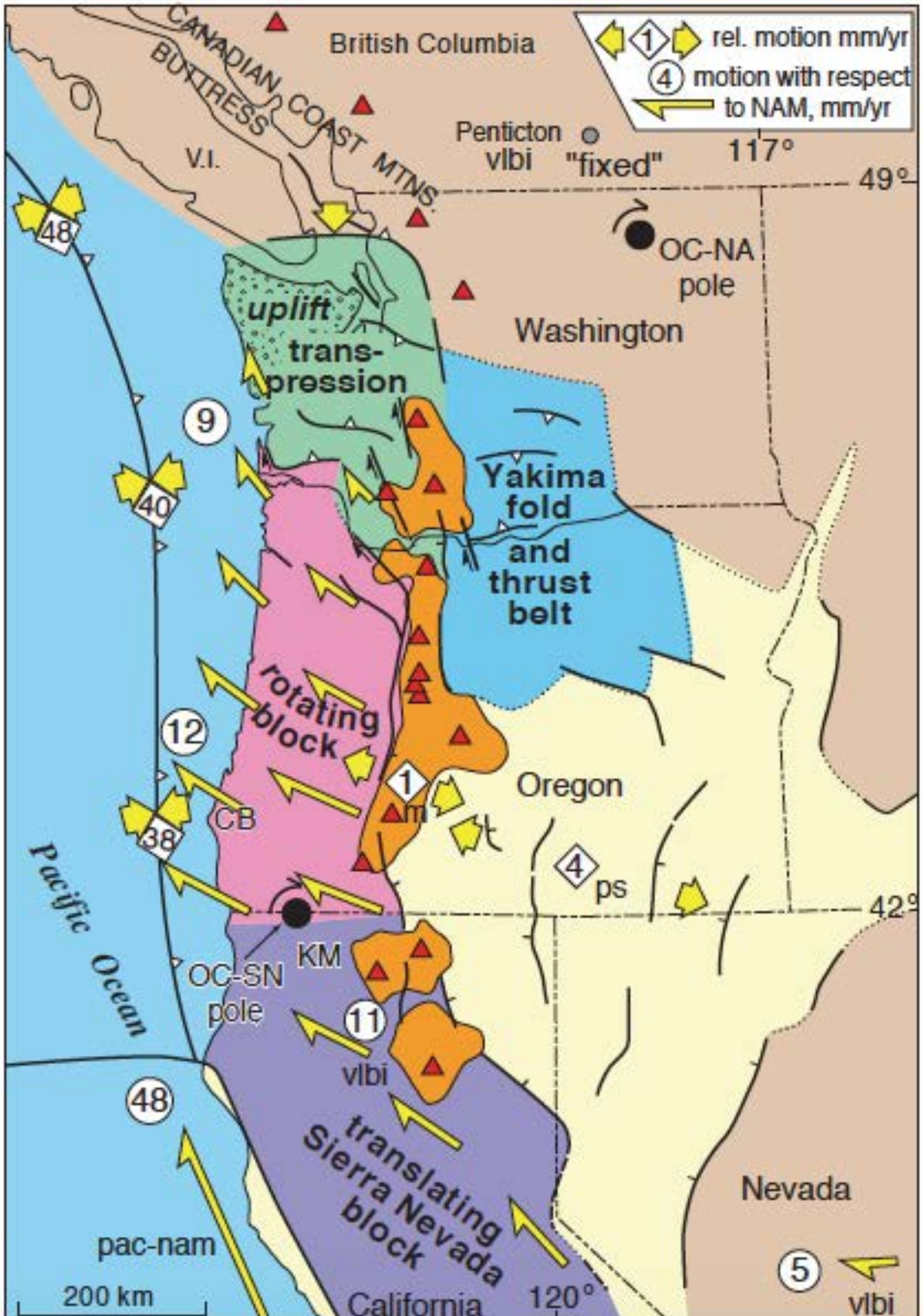

Figure 4. Velocity field for Cascadia fore arc calculated from OC-NA pole. Oregon block (pink) rotating at Neogene paleomagnetic rate is linked to Sierra Nevada block moving at vlbi rate by Euler pole (OC-SN) in Klamath Mountains (KM). Extensional arc forms along trailing edge of Oregon fore-arc block which absorbs Sierra Nevada displacement by rotating over trench at Cape Blanco (CB). North end of Oregon block deforms Washington fore arc (green) against Canadian buttress, causing north-south compression, uplift, thrust faulting, and earthquakes. Rates from very long baseline interferometry (vlbi); paleoseismology (ps); magmatic spreading (m); Pacific–North America motion (pac-nam); other symbols as in Figure 1.

The Coast Range: Tyee Basin and Siletzia

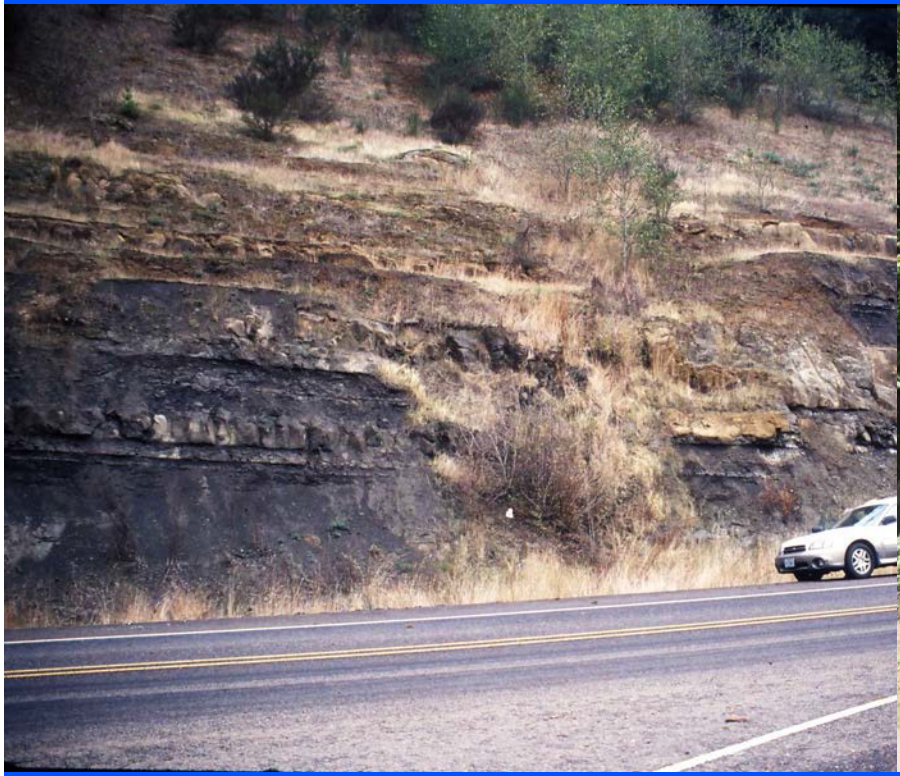


Tyee & Other Sediments

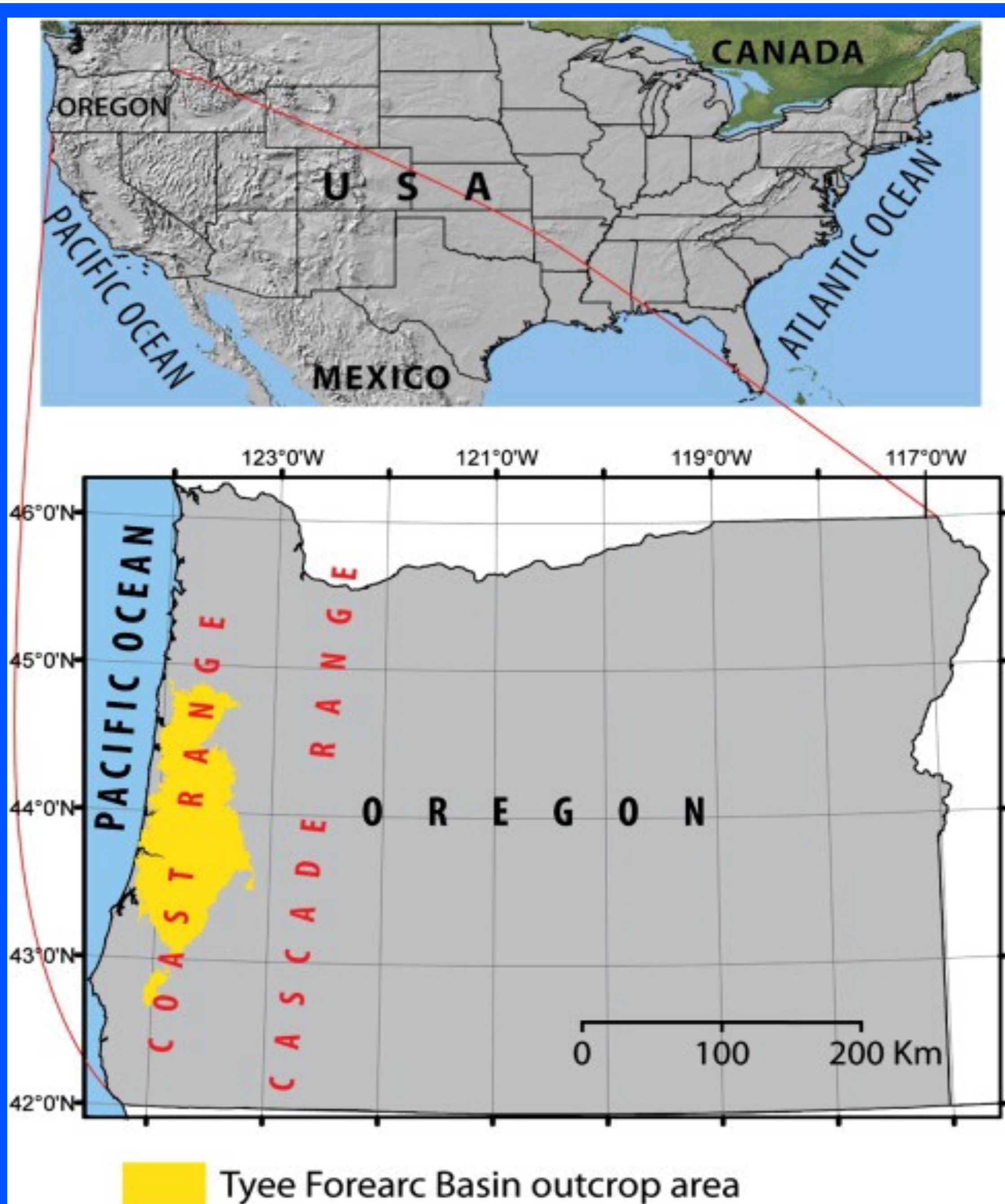

Santra et al 2013 Global and Planetary Change, Volume 103, 2013, 207 - 231

The Tyee Basin

What is the nature of the sedimentary basin?

What is the tectonic setting of the basin?

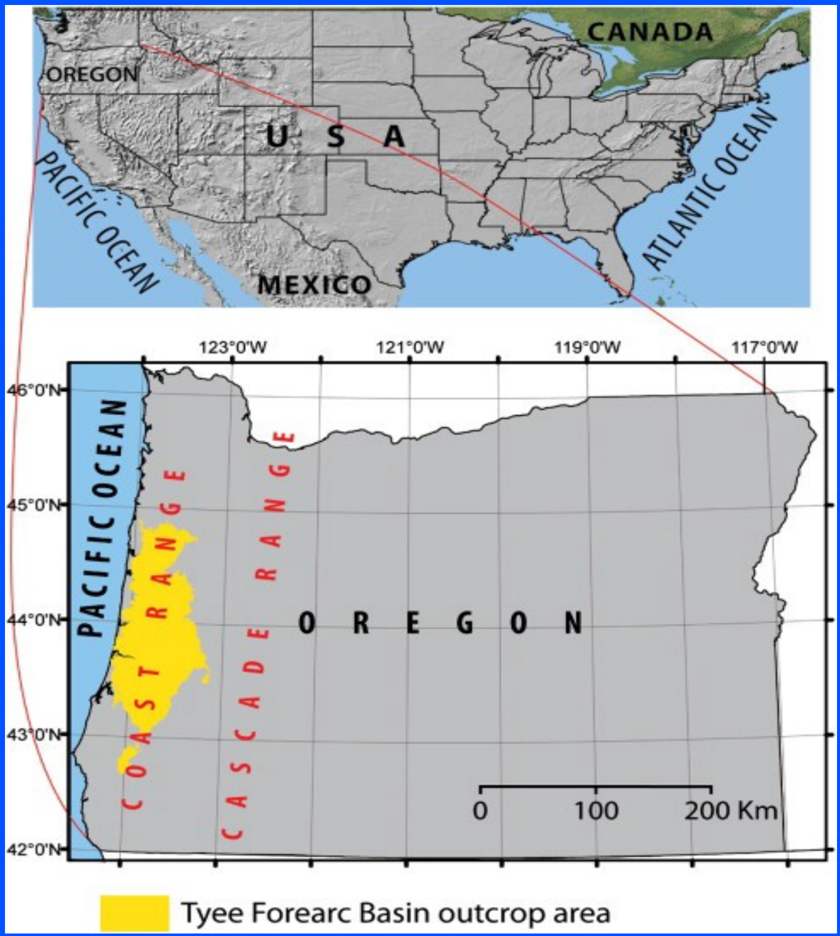

Santra et al 2013 Global and Planetary Change, Volume 103, 2013, 207 - 231

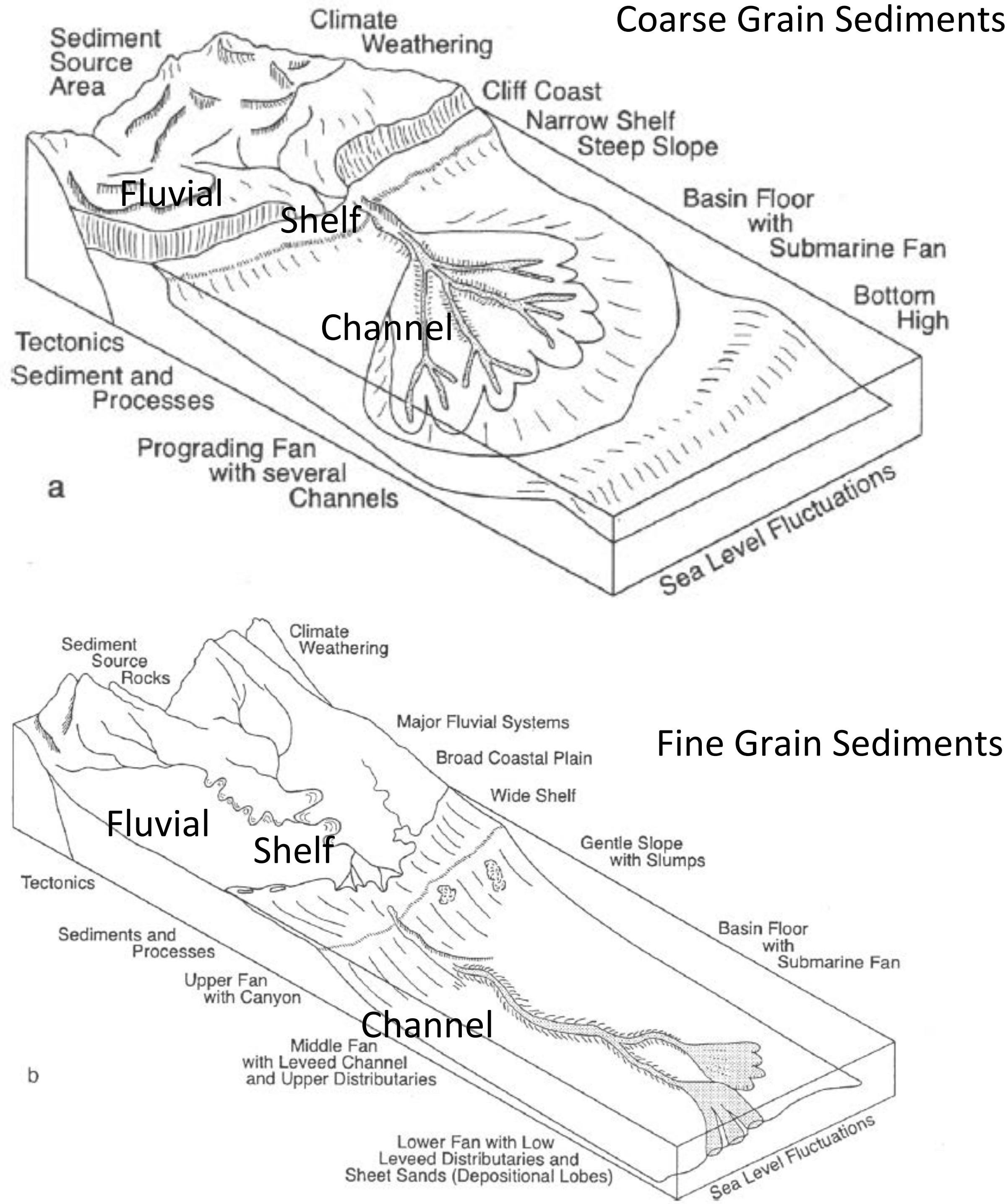

Fig. 1. Schematic block diagrams showing two end models with different relative distances from the sediment-producing mountains, to the coast, the relative width of the shelf, and the shape and location of the submarine fan. Major forces that produce transport and deposit sediment are mentioned. Morphological differences are shown. (**a**) Typical situation for coarse-grained/sand-rich fans fans; (**b**) for fine-grained/mud-rich fans. Based on Stow *et al.* (1985), Reading & Richards (1994) and Bouma (2000a,b).

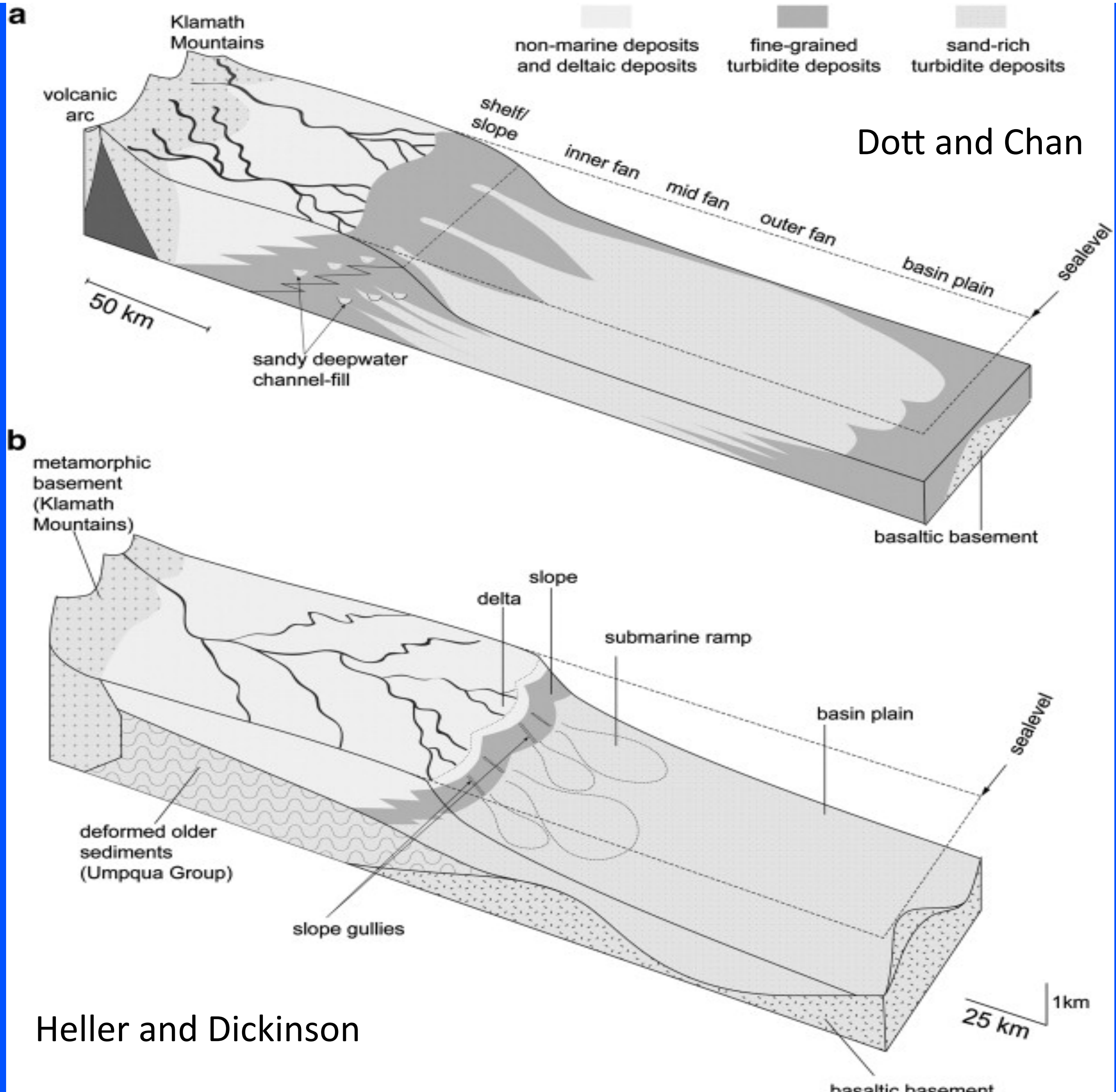

Fig. 2 Pre-existing depositional models for Tyee Forearc Basin

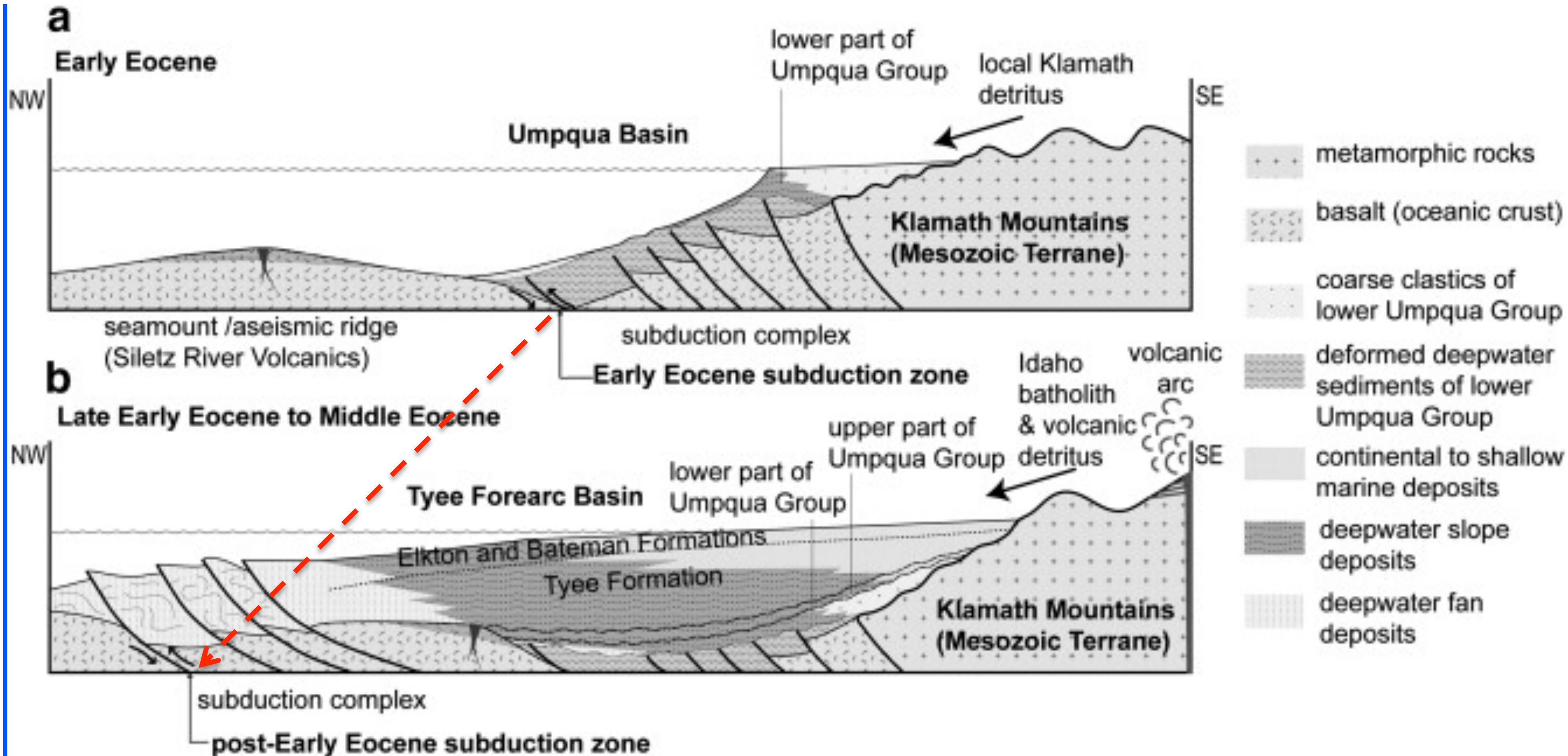

Fig. 4 Depo-tectonic model for the Tyee forearc Basin. a. Early Eocene subduction and deposition of the Umpqua Group. b. Arresting of subduction along early Eocene trench and formation of a new subduction zone in late Early Eocene

Santra et al 2013 Global and Planetary Change, Volume 103, 2013, 207 - 231

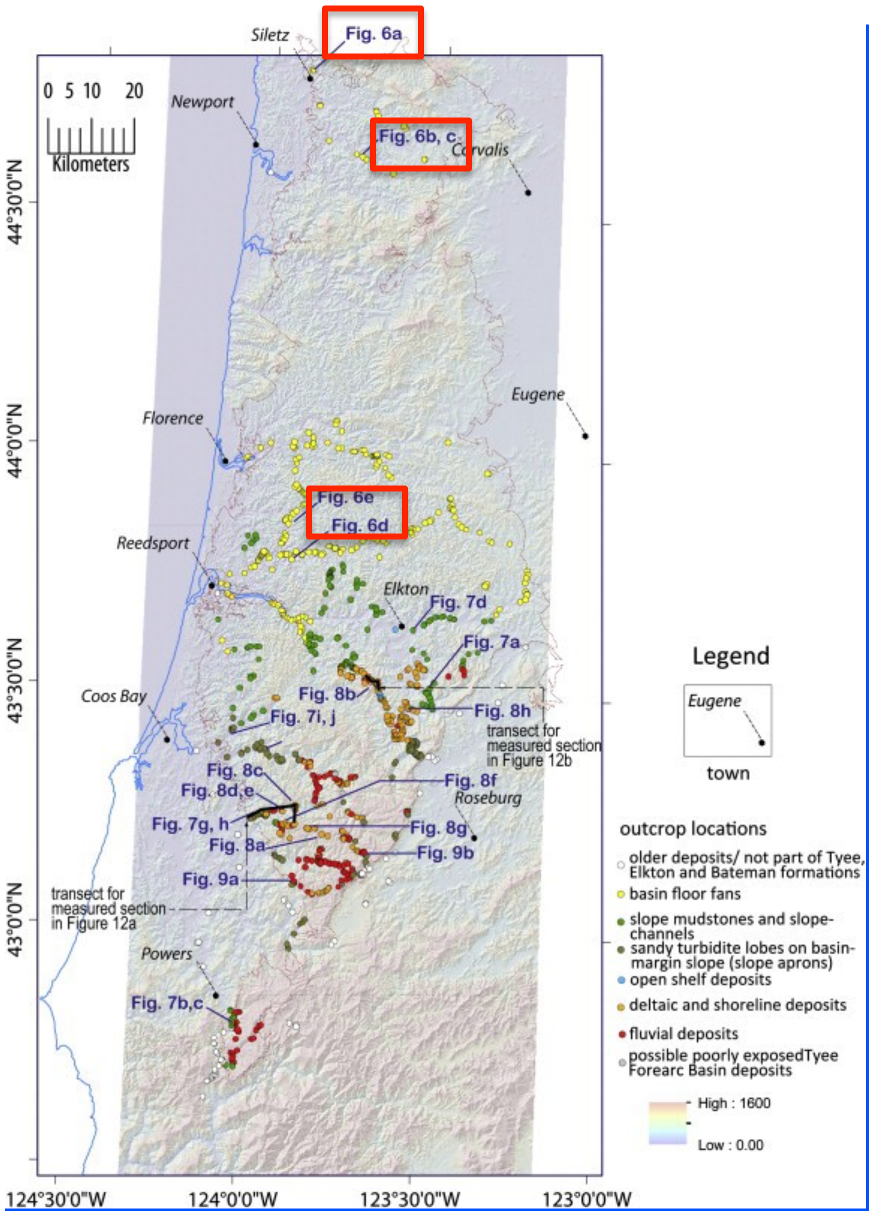

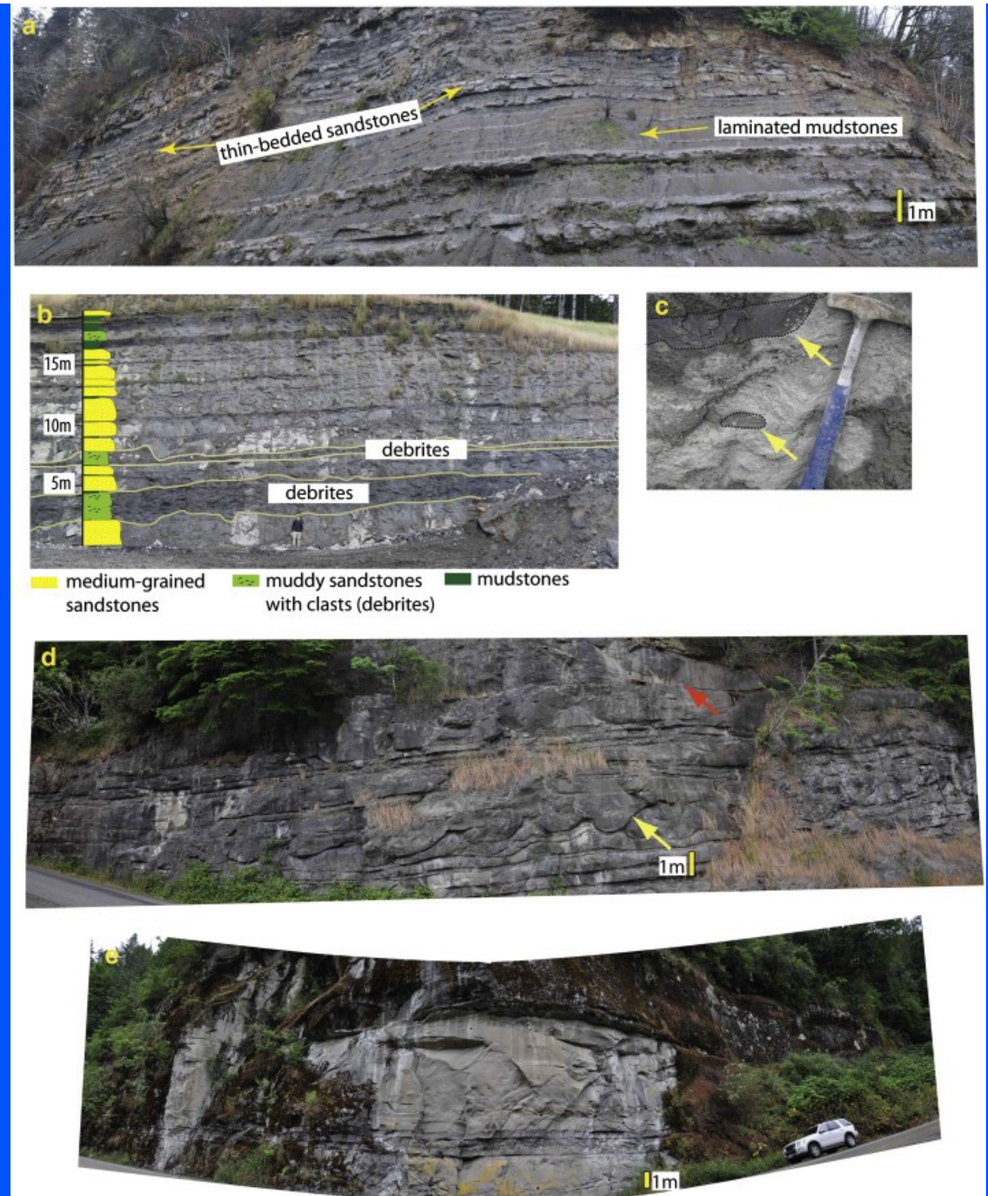

Fig. 6 Unconfined turbidite deposits of central and northern Tyee Forearc Basin — proximal and distal deepwater fan deposits;

Santra et al 2013 Global and Planetary Change, Volume 103, 2013, 207 - 231

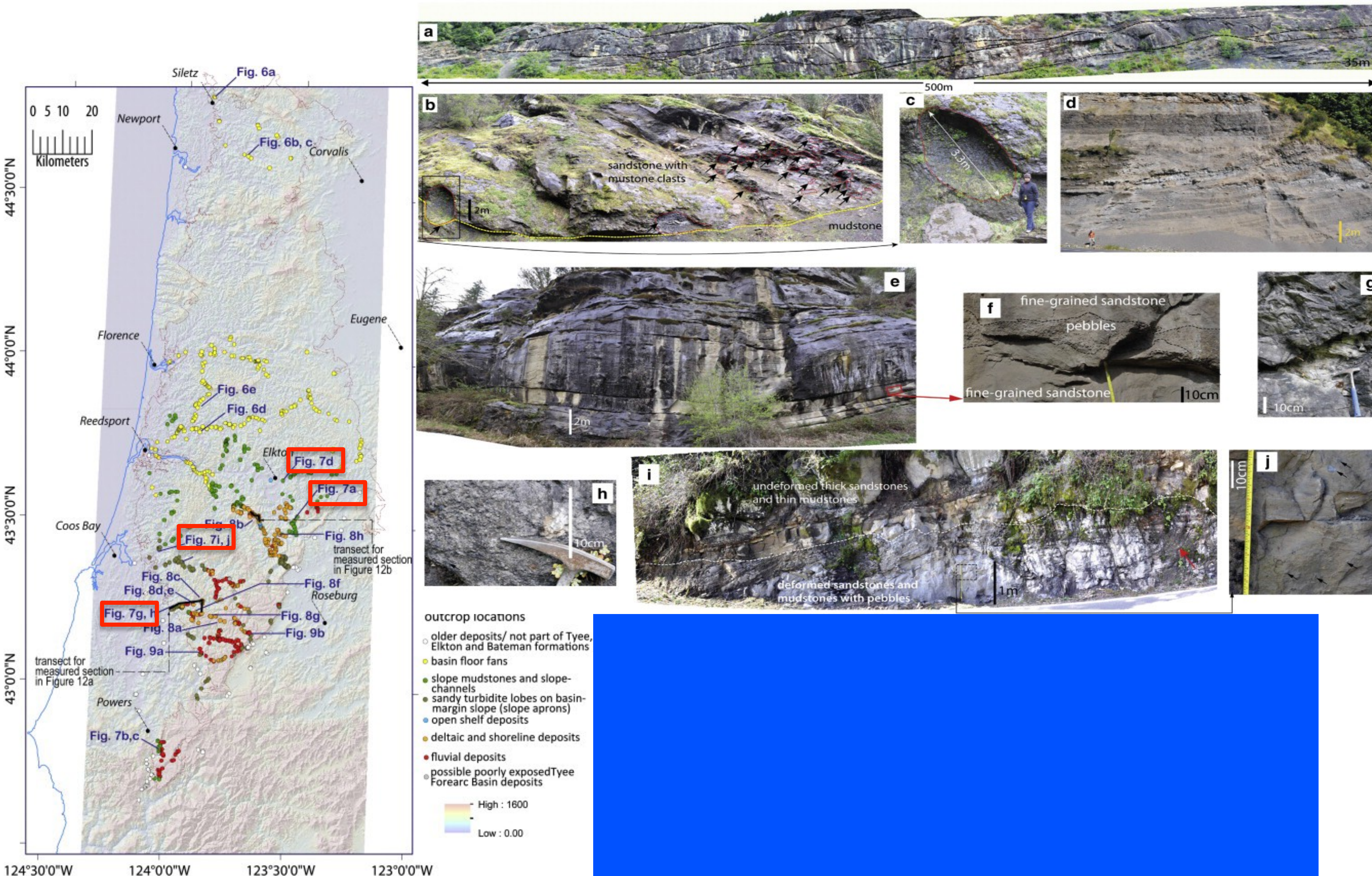

Fig. 7 Outcrop examples of channelized turbidite deposits (panels a–c), laterally extensive fine-grained slope turbidites of central Tyee Forearc Basin (panel d), and unconfined sandy turbidite deposits of southern Tyee Forearc Basin

Santra et al 2013 Global and Planetary Change, Volume 103, 2013, 207 - 231

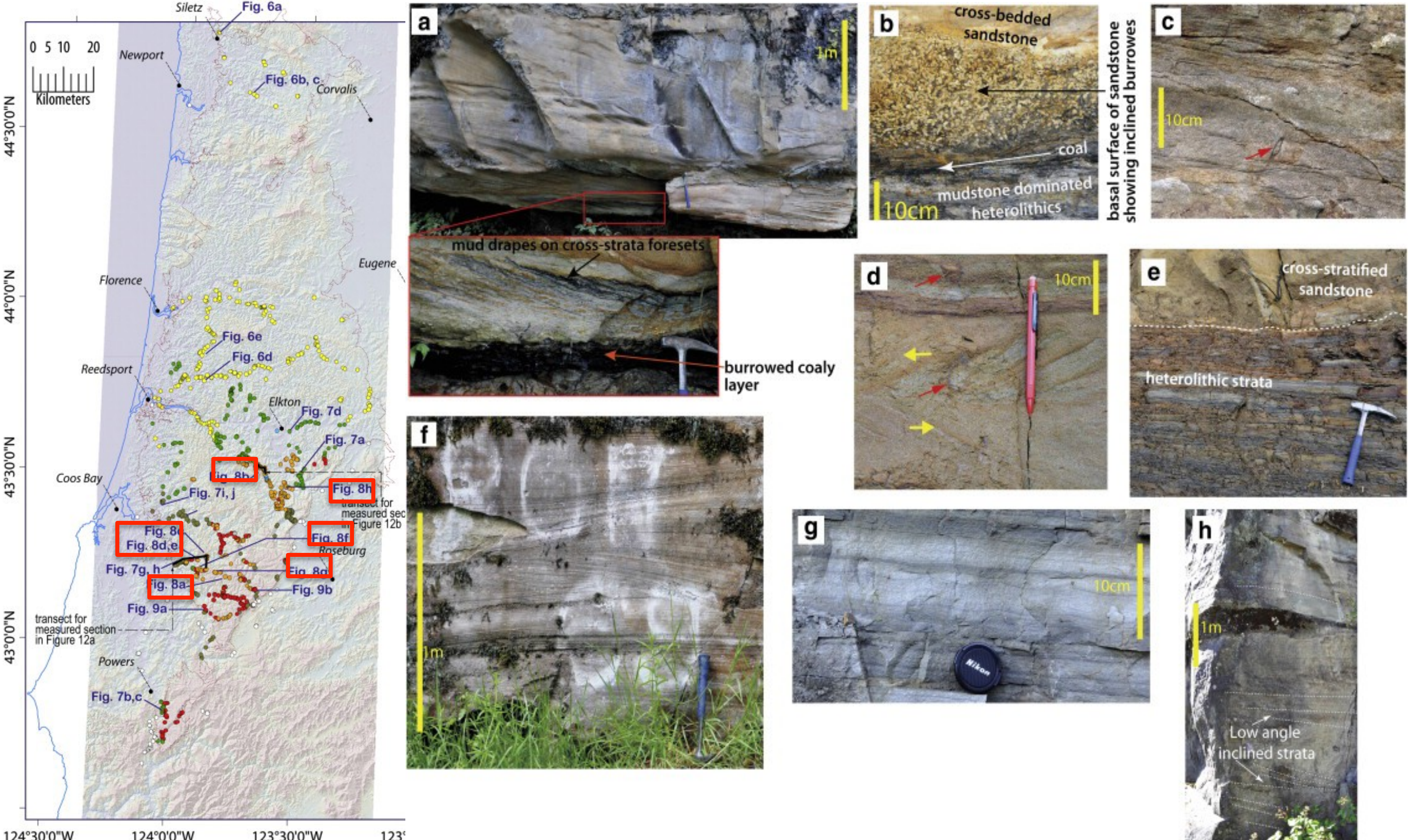

Fig. 8 Shallow marine deposits with strong tidal influence (a–e) and wave influence (f–h); for lithofacies types (L) and lithofacies associations (FA) shown in the figure

Santra et al 2013 Global and Planetary Change, Volume 103, 2013, 207 - 231

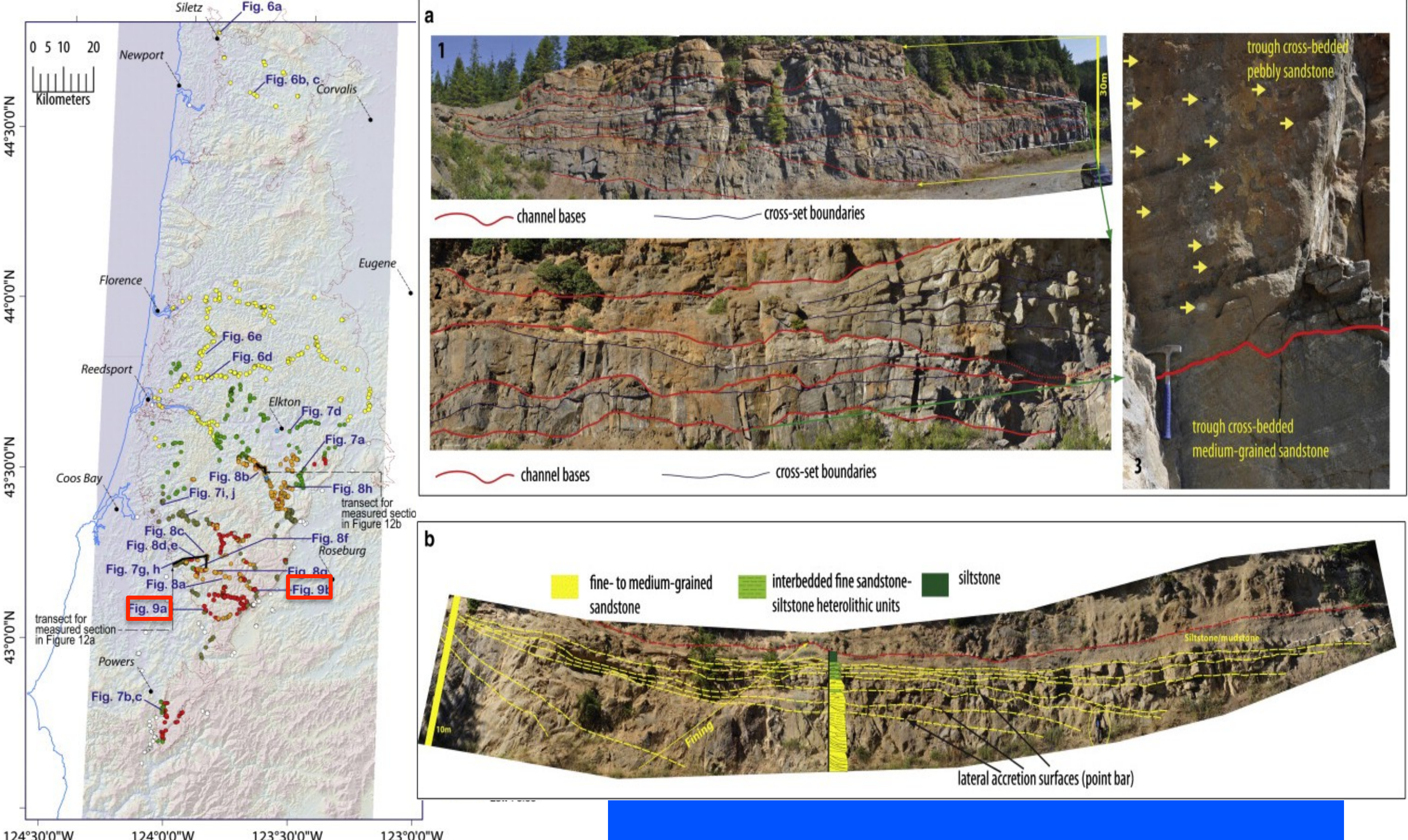

Fig. 9 Outcrop examples of fluvial deposits — southern Tyee Forearc Basin; coarse-grained braided river deposit with pebbles (Fig. a-1, 2, 3), and fining upward pointbar deposits with associated muddy flood-plain deposits (panel b).

Santra et al 2013 Global and Planetary Change, Volume 103, 2013, 207 - 231

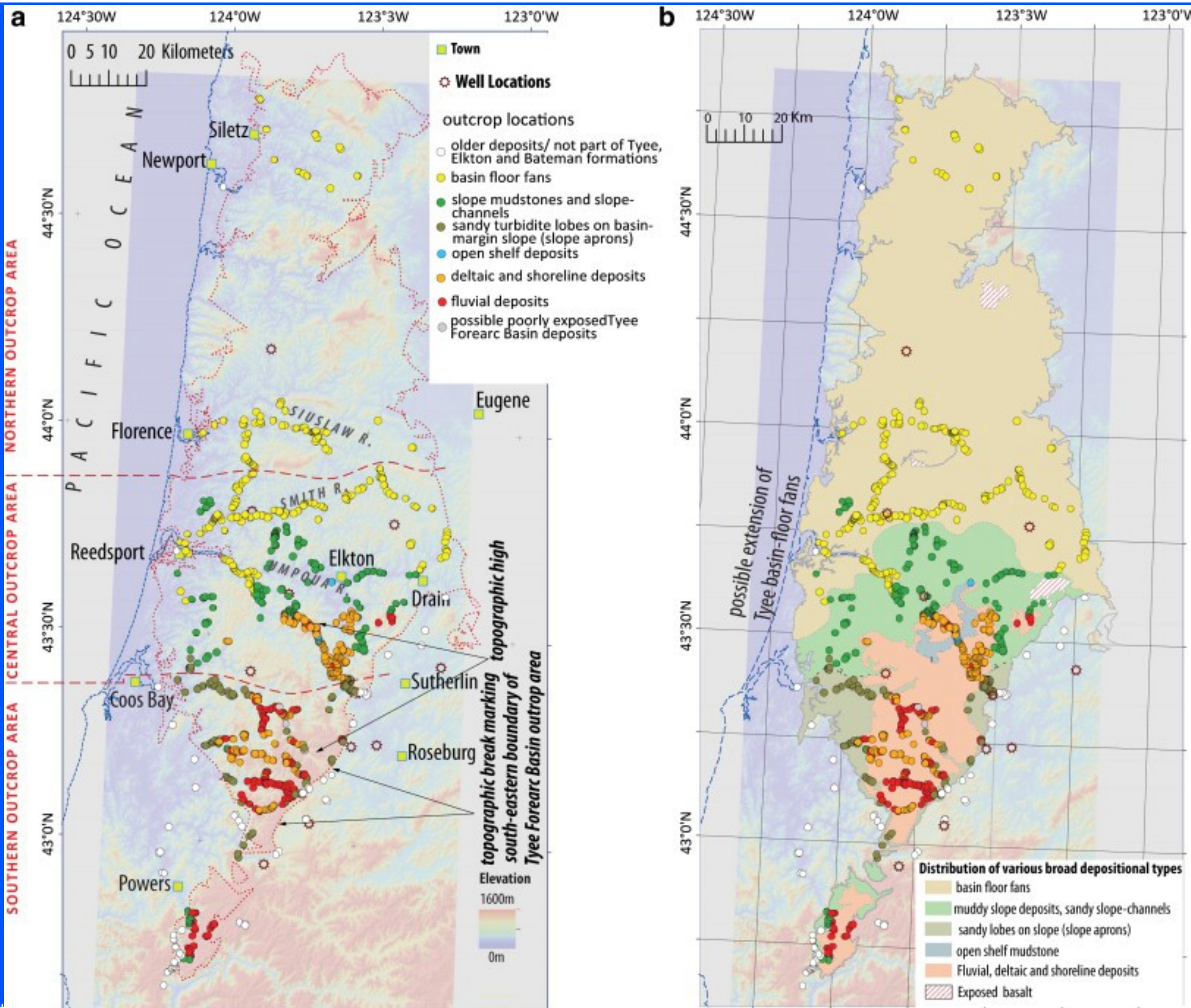

Santra et al 2013 Global and Planetary Change, Volume 103, 2013, 207 – 231

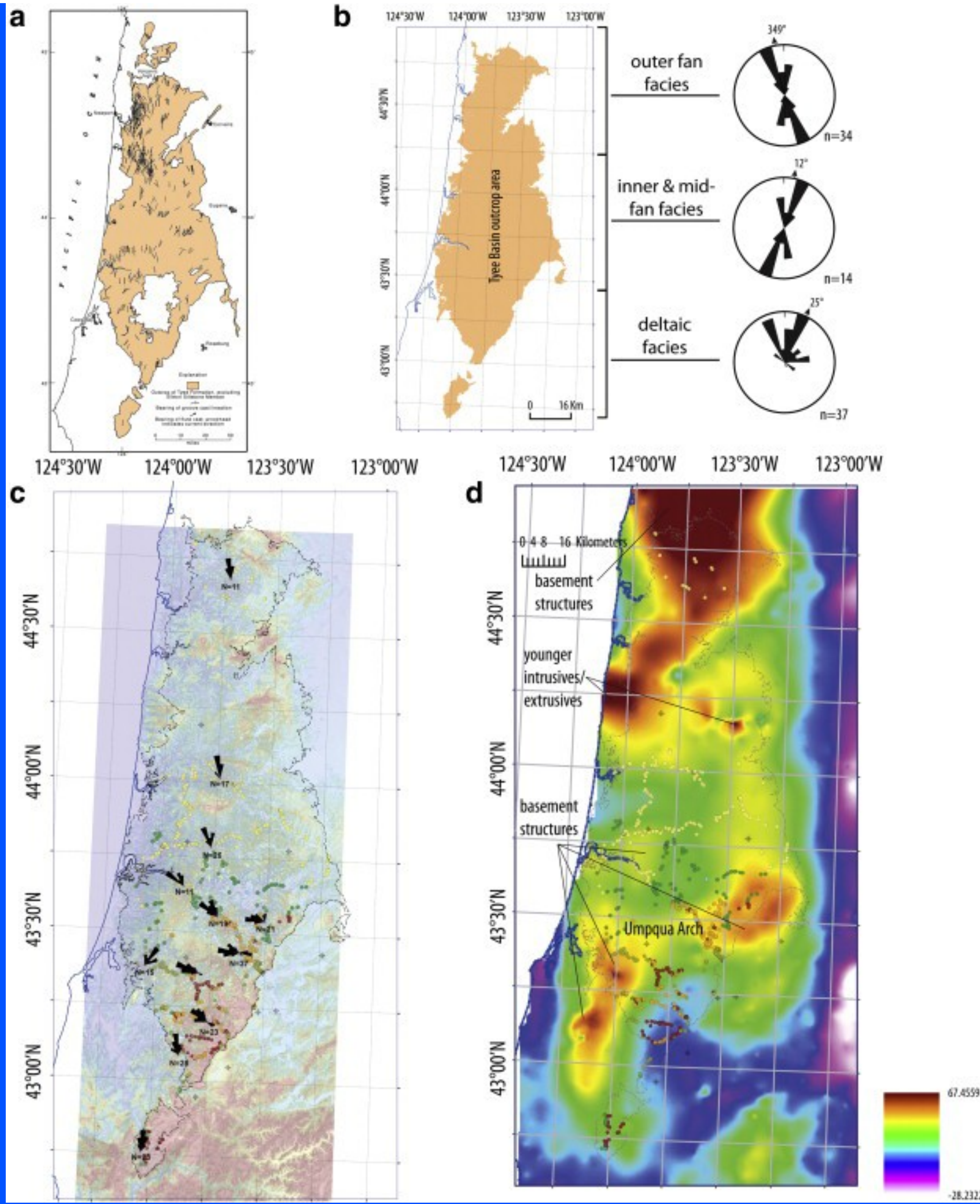

Santra et al 2013 Global and Planetary Change, Volume 103, 2013, 207 - 231

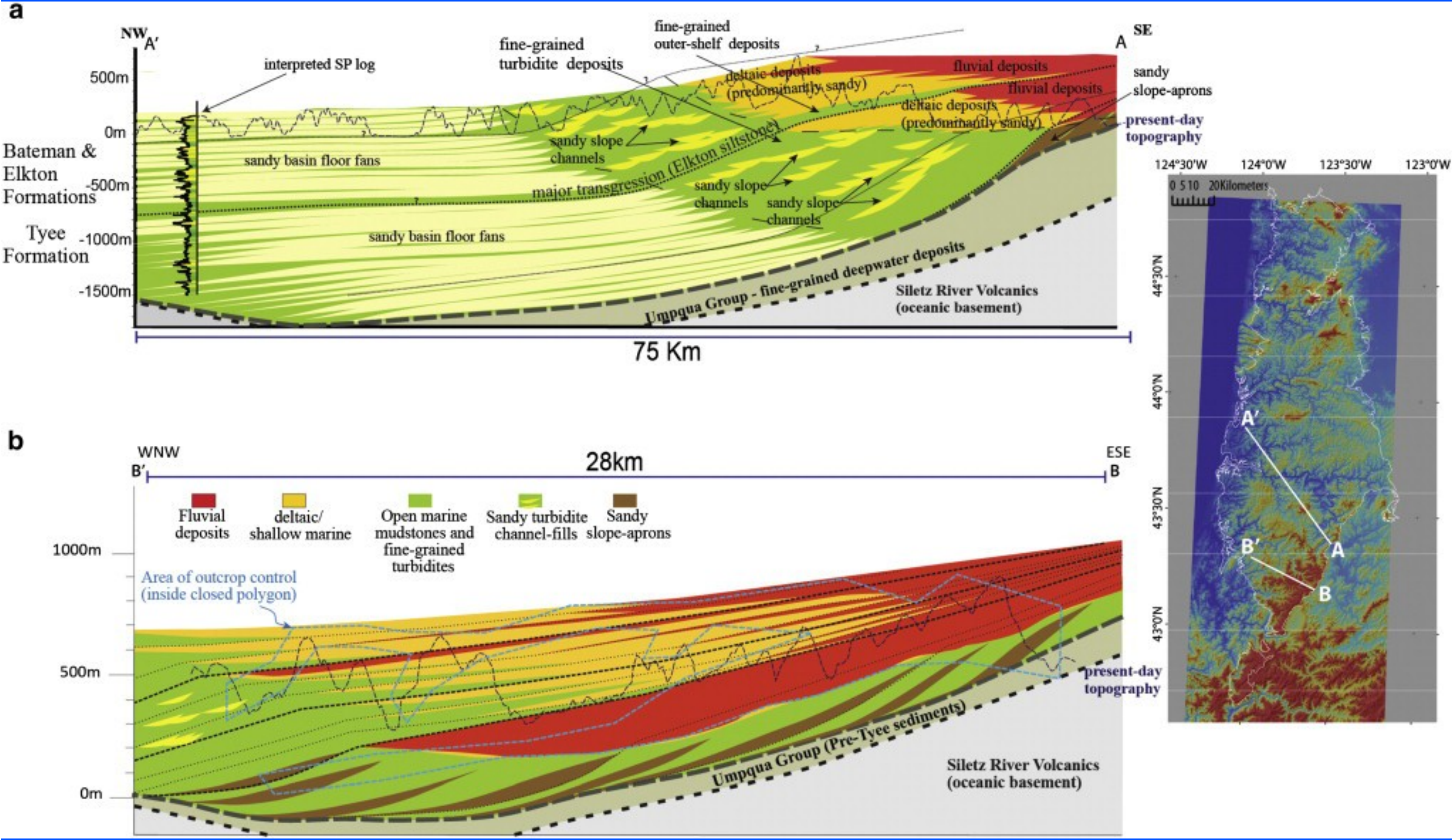

Santra et al 2013 Global and Planetary Change, Volume 103, 2013, 207 - 231

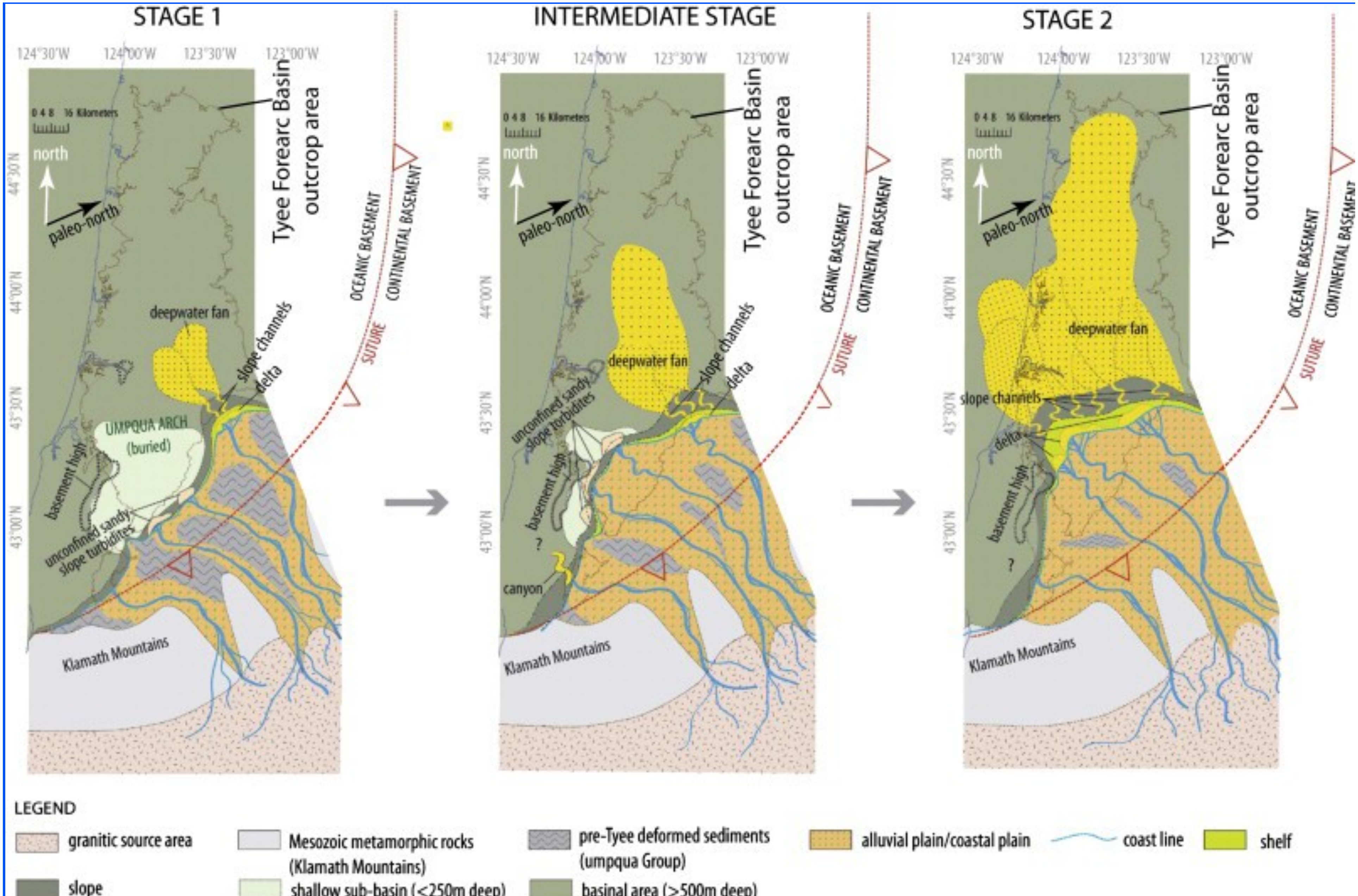

Santra et al 2013 Global and Planetary Change, Volume 103, 2013, 207 - 231

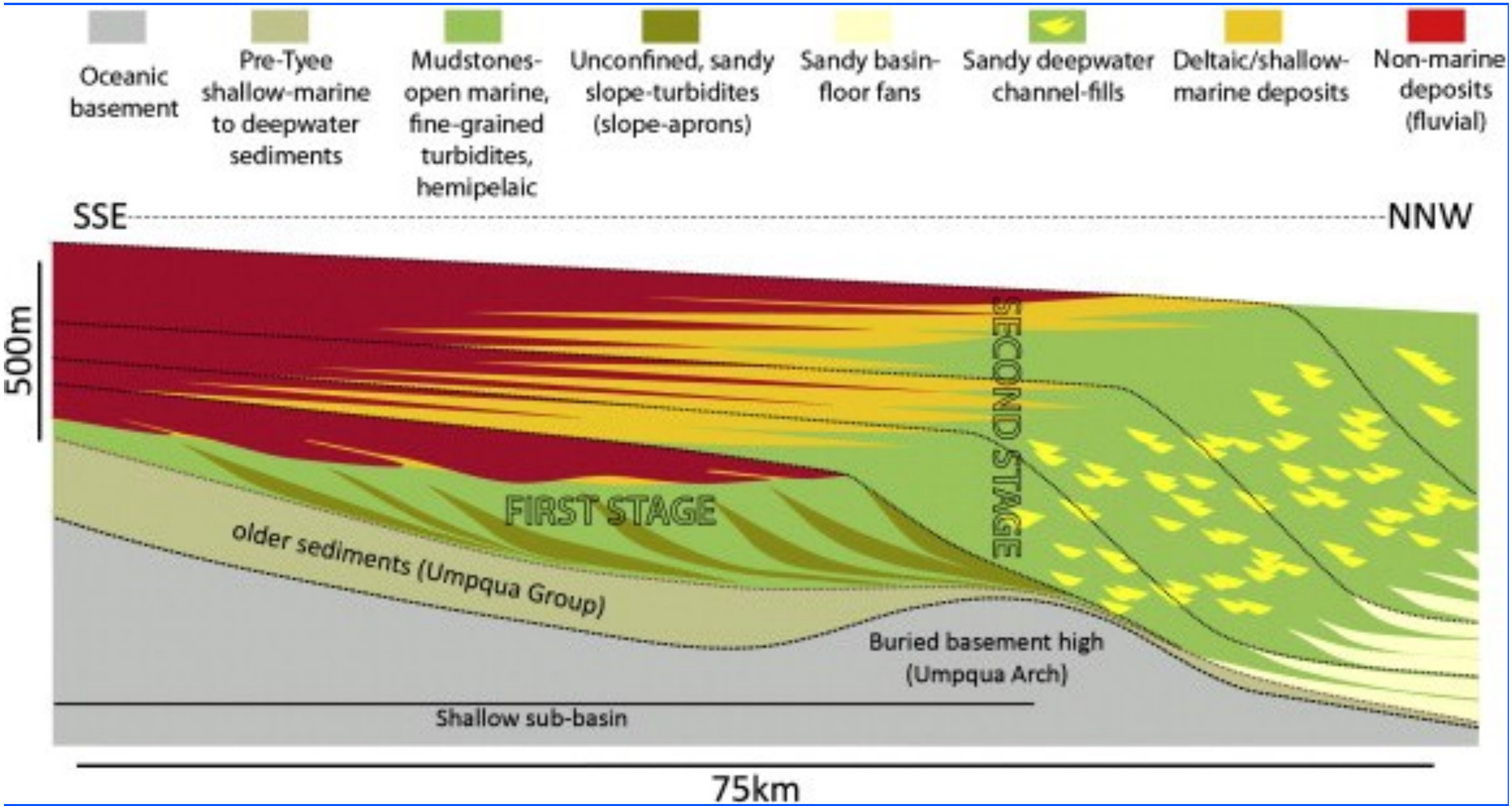

Santra et al 2013 Global and Planetary Change, Volume 103, 2013, 207 - 231

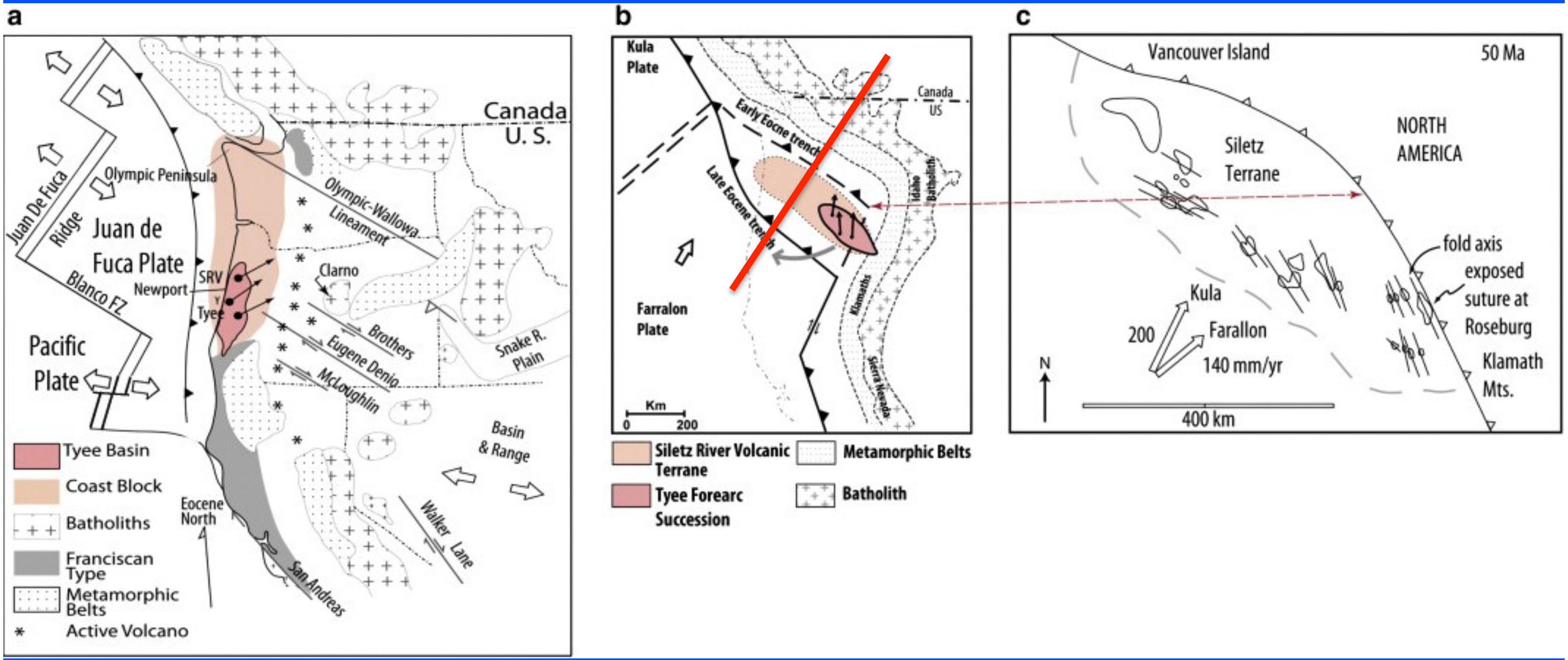

Fig. 3 Some important tectonic elements of the present-day western North America and a model for accretion and post-Early Eocene rotation of Siletz River Volcanics (SRV).

Santra et al 2013 Global and Planetary Change, Volume 103, 2013, 207 - 231

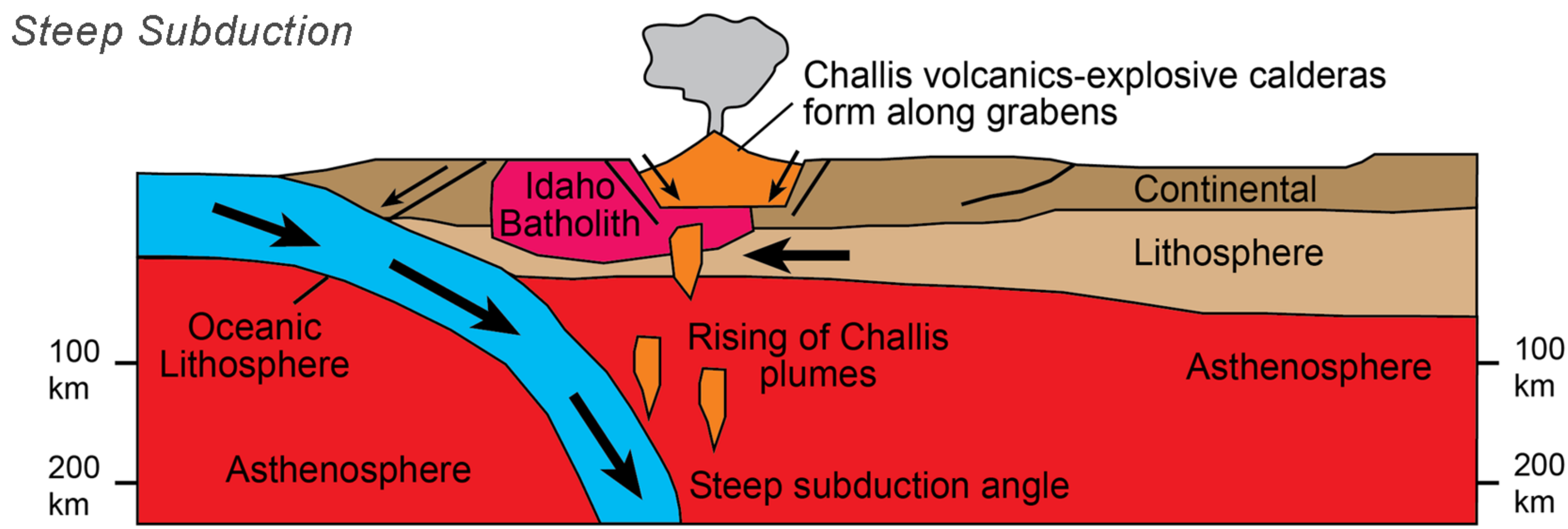

~ 50 Ma, Challis time

Tillamook & Other Volcanics

Tillamook Volcanics Outcrop
Fault Plane
Nehalem River
NB slickensides

Siletz Volcanics south of Cape Perpetua, Oregon


Basalt flow near summit, Cape Perpetua, Oregon


Siletz Volcanics dike, Cape Perpetua, Oregon

Cape Perpetua, Oregon: Eocene Siletz Volcanics

Siletzia Revisited

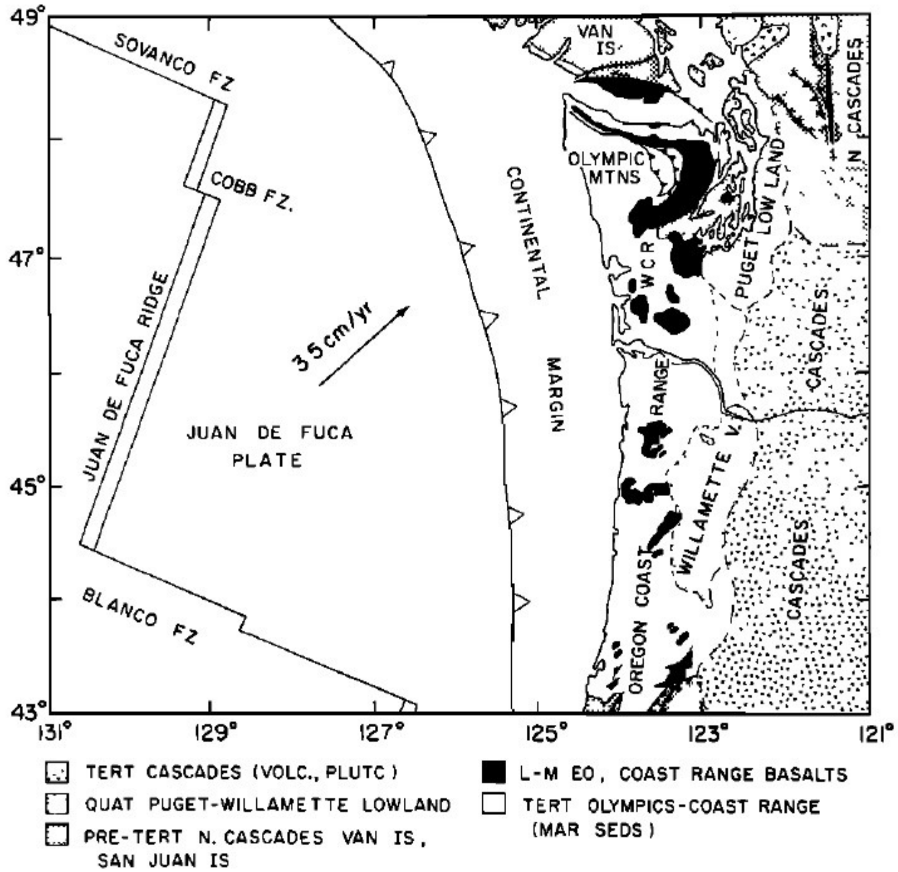

Fig. 1. Generalized geology and present plate boundaries in the Pacific Northwest. The basement rocks in the Coast Range (solid black) crop out in a north-south linear pattern from the southern tip of Vancouver Island to southern Oregon. These are tholeiitic submarine pillow lavas and subaerial alkalic basalts, which are thought to have been erupted as a line of islands at a segment of the early Tertiary Farallon-Kula plate spreading ridge.

R A Duncan 1982
A Captured Island Chain in the Coast Range of Oregon and Washington

JGR v 87, B13, 10827-10837

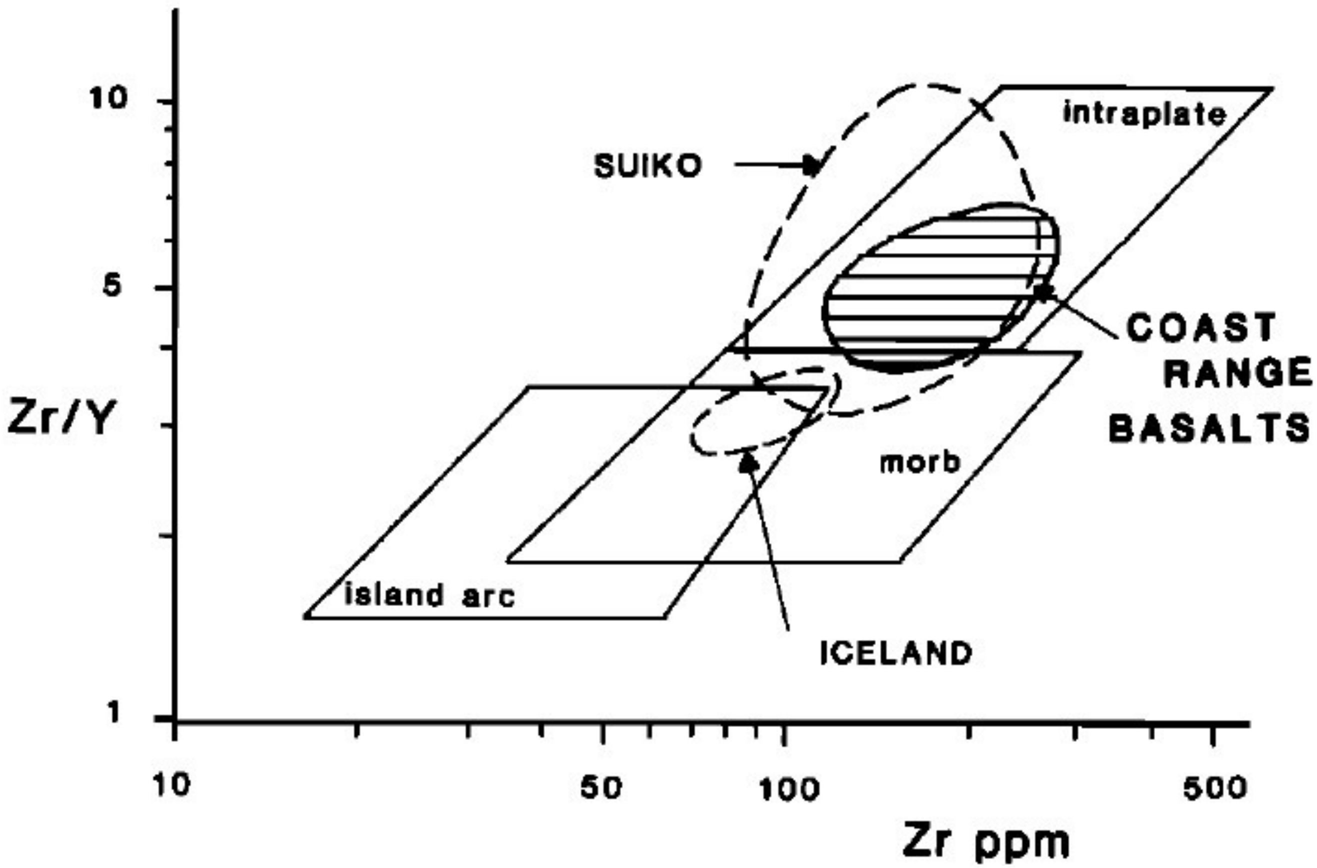

Fig. 5. Trace elements have been used to distinguish the tectonic environment of eruption of otherwise similar basalts. Here Zr and Y are used to characterize basalts from the Coast Range [Loeschke, 1979; Globerman, 1980] as intraplate to ocean floor origin. For comparison, analyses from Suiko Seamount [Kirkpatrick et al., 1981] and eastern Iceland [Wood, 1978] are illustrated.

Duncan 1982

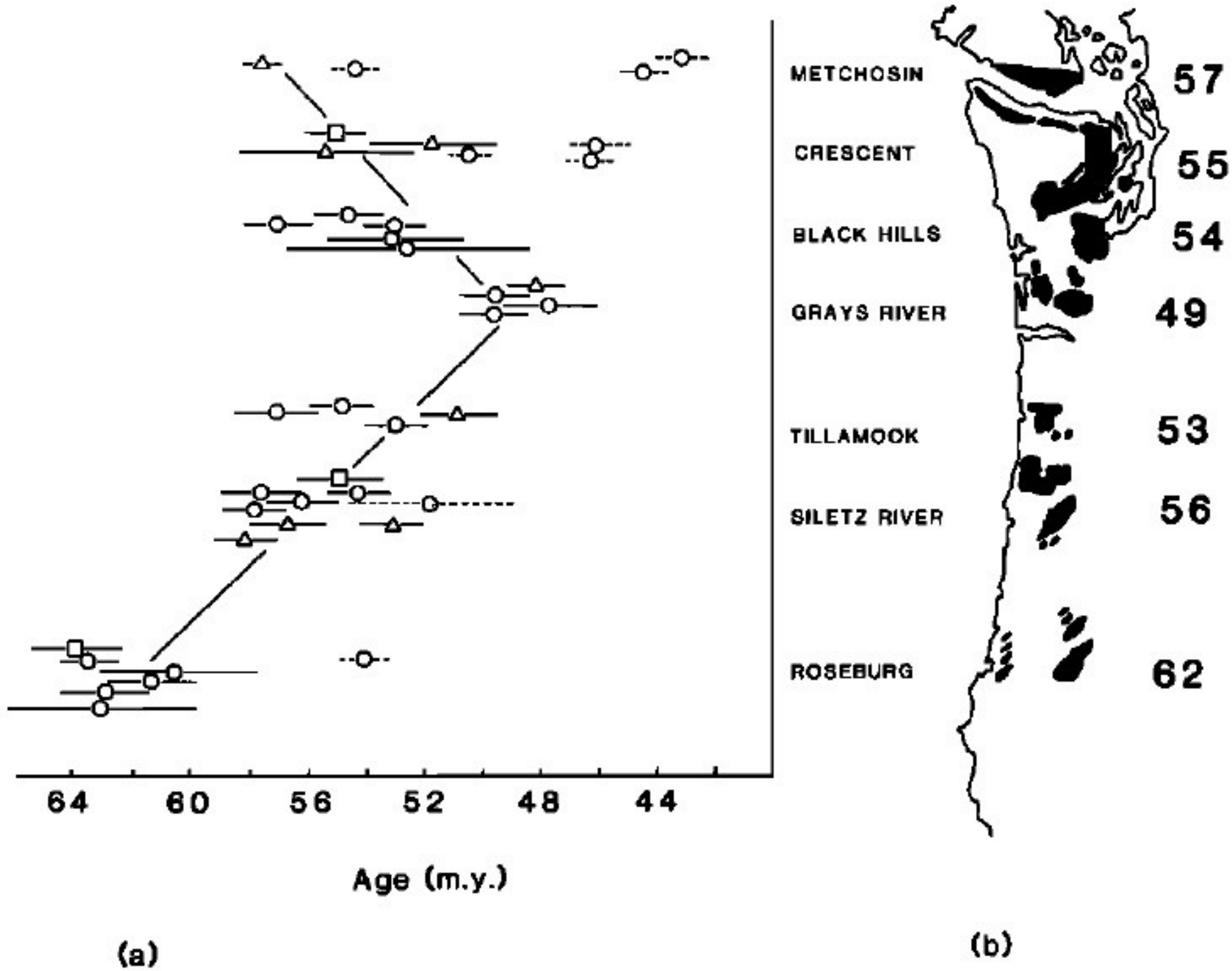

Fig. 2. (a)K-Ar and $^{40}Ar-^{39}Ar$ geochronology of basalts from the Coast Range, Oregon and Washington, reveals a V-shaped pattern when ages at various eruptive centers are plotted against distance. Open circles are conventional K-Ar

Duncan 1982

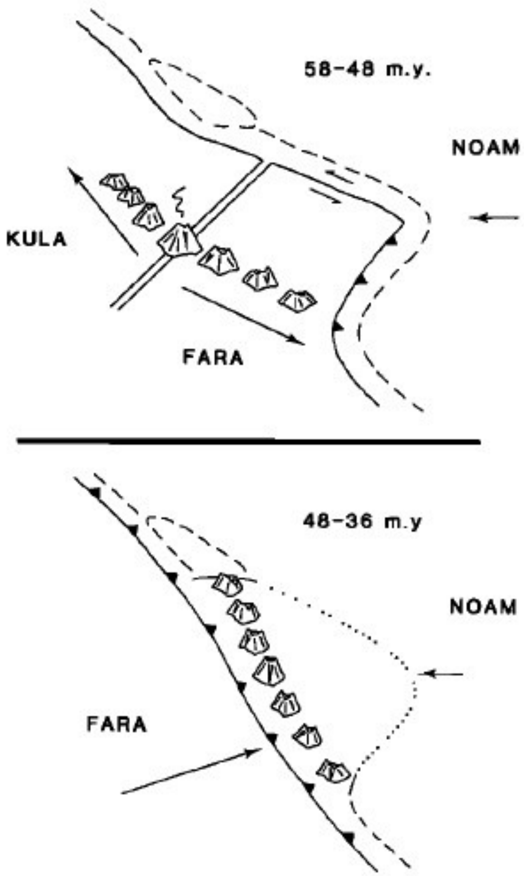

Fig. 4. (top) The distribution of ages within the early Tertiary eruptive centers favors an origin by hot spot volcanism underlying a spreading ridge segment. Seamounts and islands so generated would have been carried away from the hot spot in two directions, on the Kula (northern Coast Range) and Farallon (southern Coast Range) plates. Calculated absolute plate motions are shown as solid arrows. (bottom) As part of a major plate motion reorganization, this ridge segment stopped spreading, succeeded by Farallon-Pacific spreading farther north, by magnetic anomaly 21 (~48 m.y.) time. The subduction zone between the Farallon and North America plates then moved to the west, capturing this island lineament against North America.

Duncan 1982

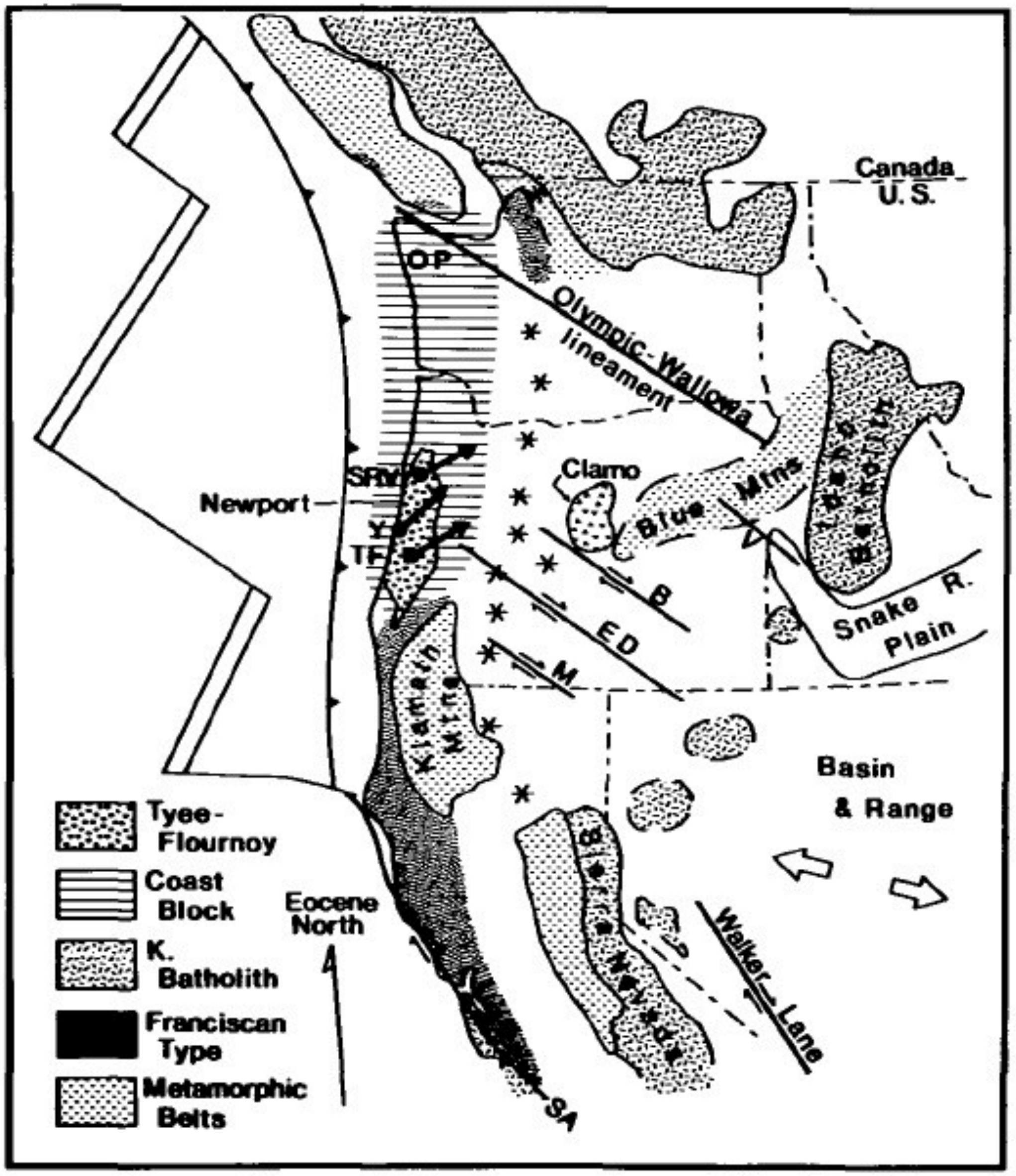

Figure 1. Generalized geologic and tectonic map of northwestern United States based in part on Hamilton (1969) and Lawrence (1976). SRV = Siletz River Volcanic Series, Y = Yachats basalt, TF = Tyee and Flournoy Formations, OP = Olympic Peninsula. Fault zones and lineaments: V = Vale, B = Brothers, ED = Eugene-Denio, M = McLoughlin, SA = San Andreas.

Simpson and Cox 1977 Paleomanetic evidence for tectonic rotation of the Oregon Coast Range *Geology* v 5, pp 585-589.

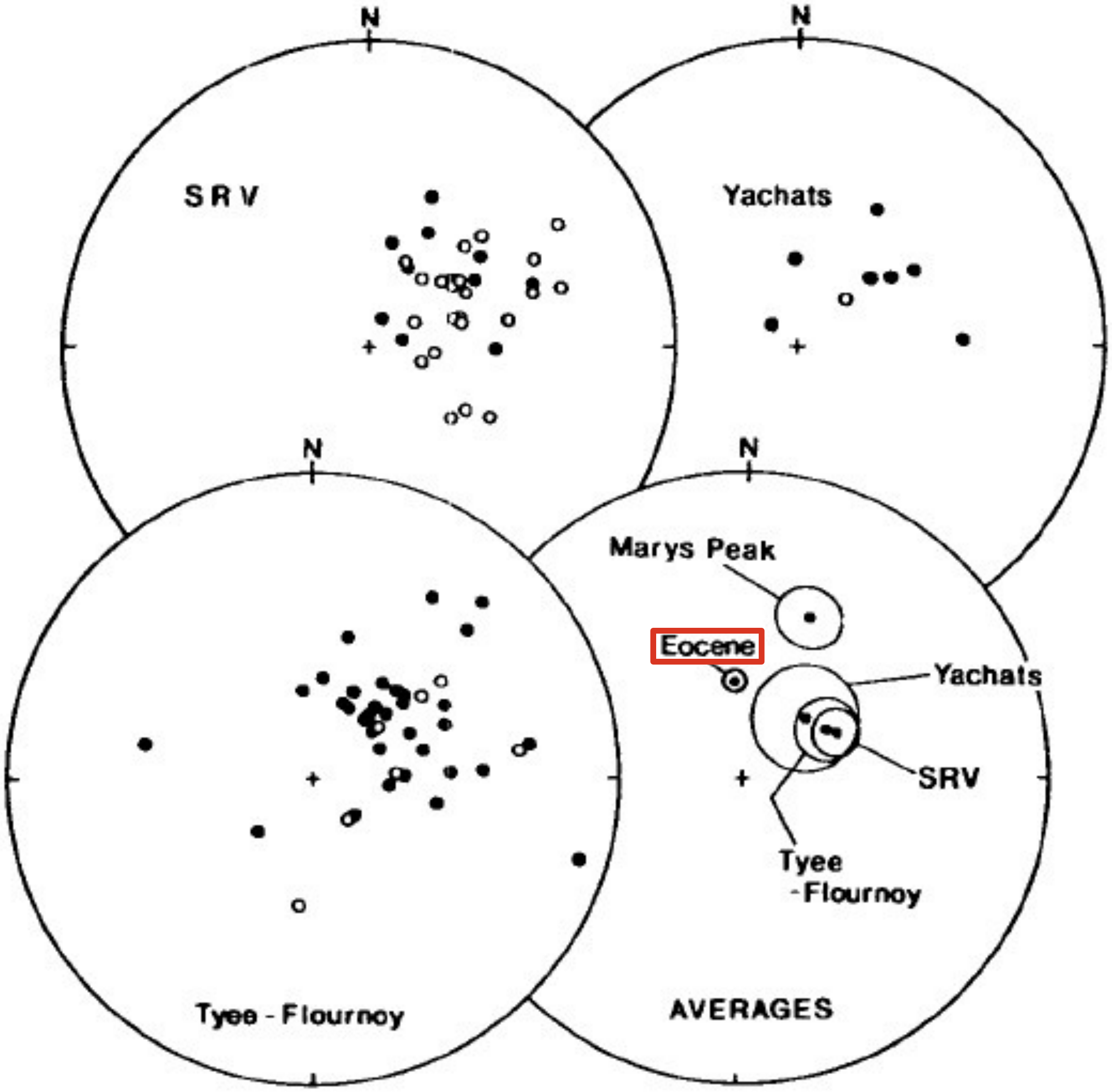

Figure 2. Site-mean magnetization directions for Siletz River Volcanic Series (SRV), Yachats basalt, Tyee and Flournoy Formations, and averages. Eocene field direction predicted from studies in stable parts of North America and result for Marys Peak sill (Clark, 1969) are also shown. Reversed polarities have been projected through origin onto lower hemisphere and are shown as open circles. Large ovals are circles of 95% confidence about the means.

Simpson and Cox 1977

TABLE 1. PALEOMAGNETIC DATA

	D (°)	I (°)	Field α_{95}	No. sites	Pole lat (°)	Pole long (°E)	Pole a_{95}	Rotation*
Expected field directions for Eocene rocks (from North American studies, see text)	355	64	4	4	87	169	6	. .
Expected field directions for Eocene rocks (from North American, European, and Russian studies, see text)	345	68	3	19	78	187	5	. .
Expected field directions for upper Tertiary rocks (Beck, 1976)	354	61	4	3	85	114	6	. .
Siletz River Volcanic Series (Cox, 1957)	70	55	7	8	37	310	9	75 ± 12
Siletz River Volcanic Series (Cox, 1959, recalculated)	68	56	7	9	39	310	9	73 ± 12
Siletz River Volcanic Series (present study)	60	62	8	24	48	306	11	65 ± 17
Siletz River Volcanic Series (Cox, 1959, recalculated, and present study)	63	61	6	33	45	307	8	68 ± 12
Tyee-Flournoy Formations	59	63	8	40	49	305	11	64 ± 16
Yachats basalt	46	64	14	8	58	308	20	51 ± 33
Marys Peak sill (Clark, 1969)	22	42	8	26	63	8	8	28 ± 12
Miocene basalts from Oregon Coast	354	52	25	8	67	349	29	0 ± 44

Note: D = declination, I = inclination.
* ± indicates 95% confidence limits.

Simpson & Cox 1977

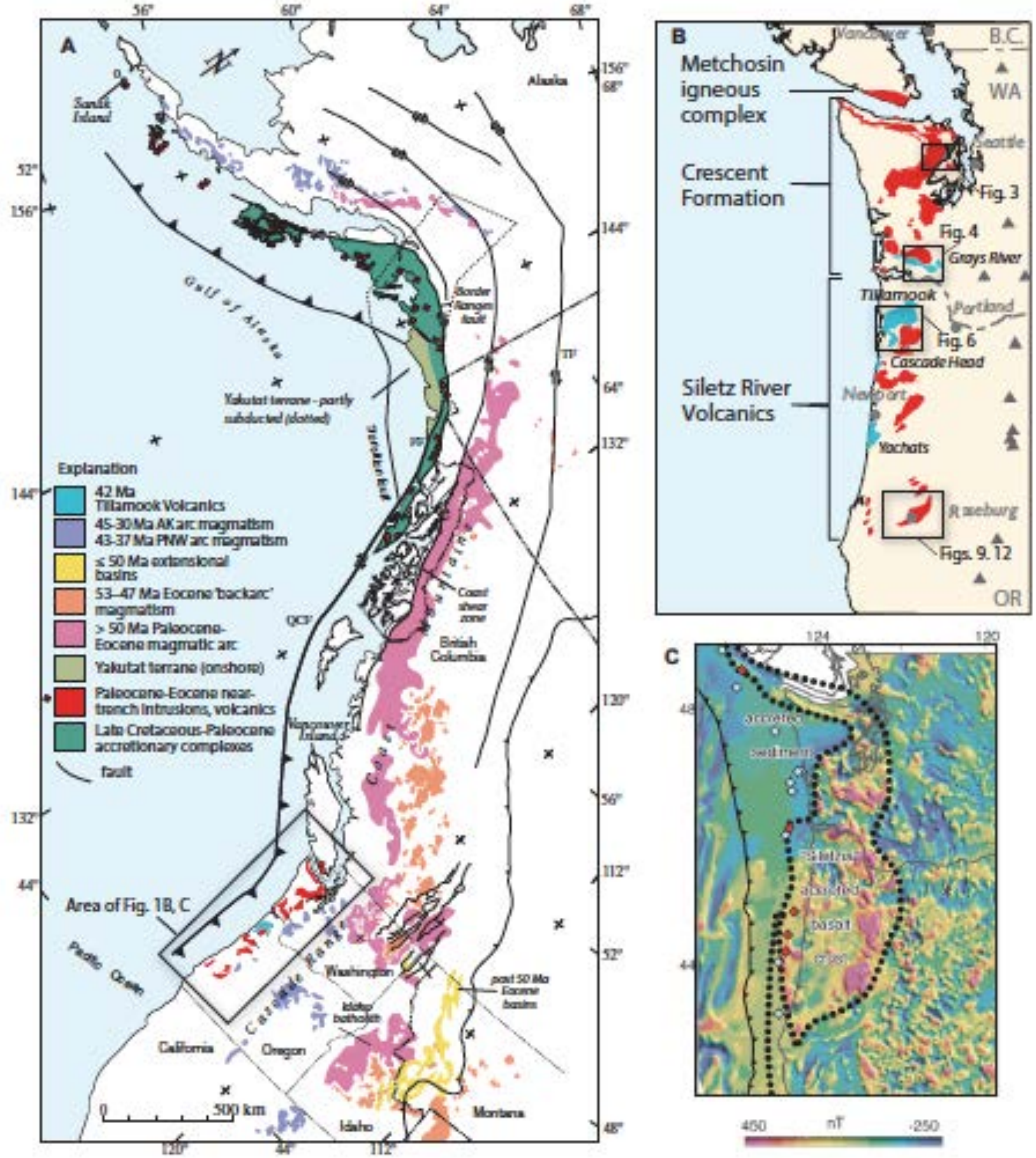

Figure 1. Tectonic setting of Siletzia. (A) Regional setting showing Paleocene–Eocene continental margin magmatism and location of oceanic Siletzia and Yakutat terranes (from Haeussler et al., 2003). FF—Fairweather Fault; QCF—Queen Charlotte Fault; TF—Tintina fault. (B) Formations composing Siletzia (red) and postaccretion basaltic magmatism (blue, from McCrory and Wilson, 2013). OR—Oregon; WA—Washington; B.C.—British Columbia. (C) Extent of Siletzia in the subsurface from regional aeromagnetic data and deep exploration wells (red bottoms in basalt, blue in sediments; from Wells et al., 1998).

Wells et al 2014

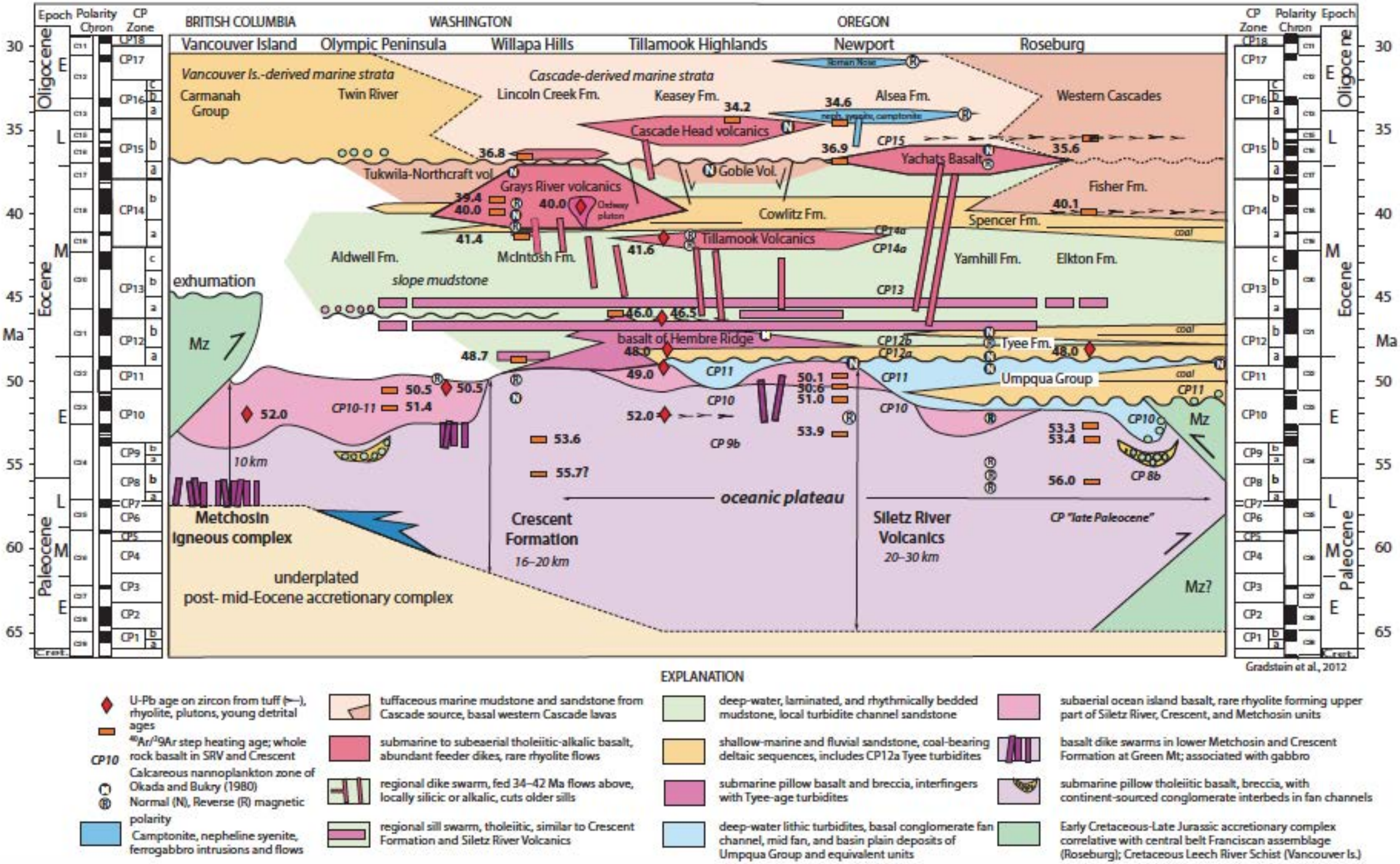

Figure 2. Siletzia time-rock diagram roughly parallel to subduction margin; time scale of Gradstein et al. (2012). Data sources: Vancouver Island geology: Yorath et al. (1999); Massey

Wells et al 2014

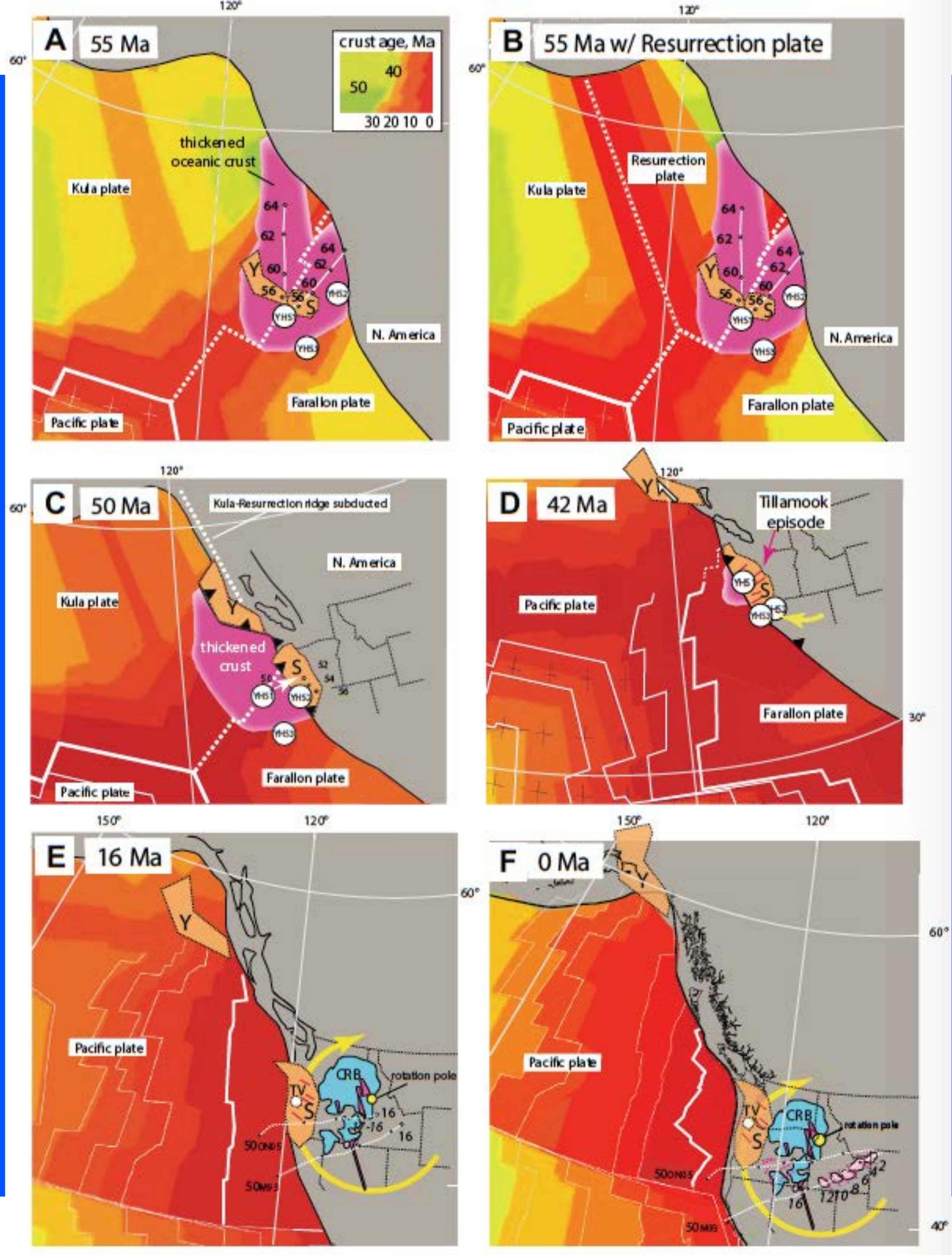

Wells et al 2014

Schmandt and Humphreys 2011

Seismically imaged relict slab from the 55 Ma Siletzia accretion

to the northwest United States

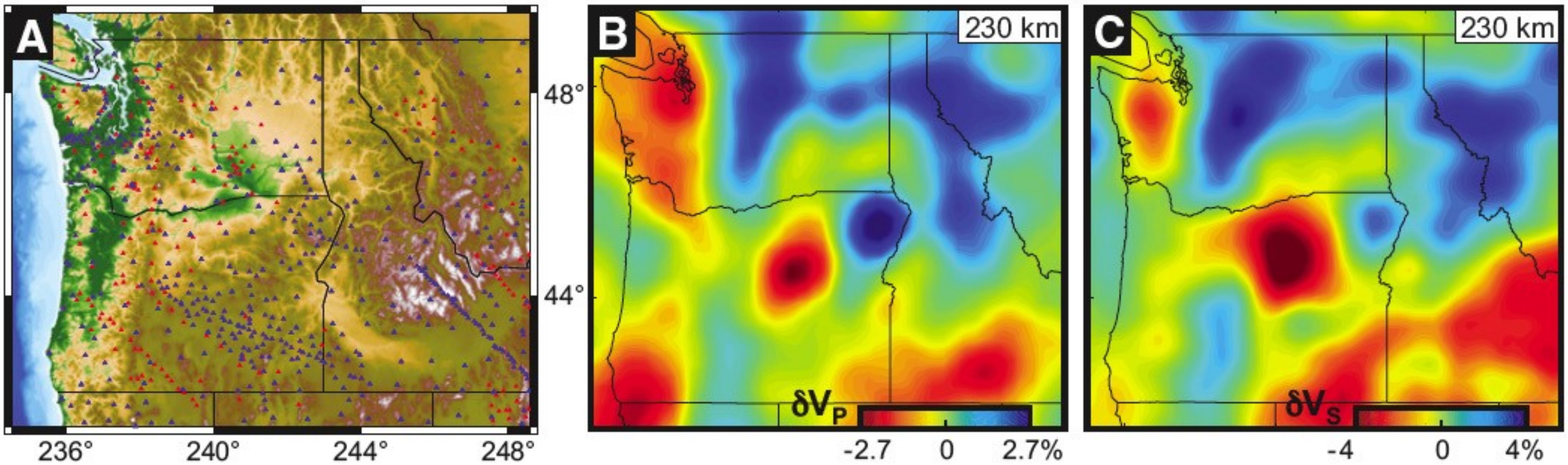

Figure 1. A: Regional topography and stations used in our study. Blue indicates stations used for P and S data; red indicates short-period stations used only for P data. Backarc area underlain by Siletzia is well approximated by low-lying Columbia basin (see Fig. 2). B: P-wave velocity variations. C: S-wave velocity variations.

Schmandt and Humphreys 2011 Seismically imaged relict slab from the 55 Ma Siletzia accretion to the northwest United States Geology v 39, p 175-178.

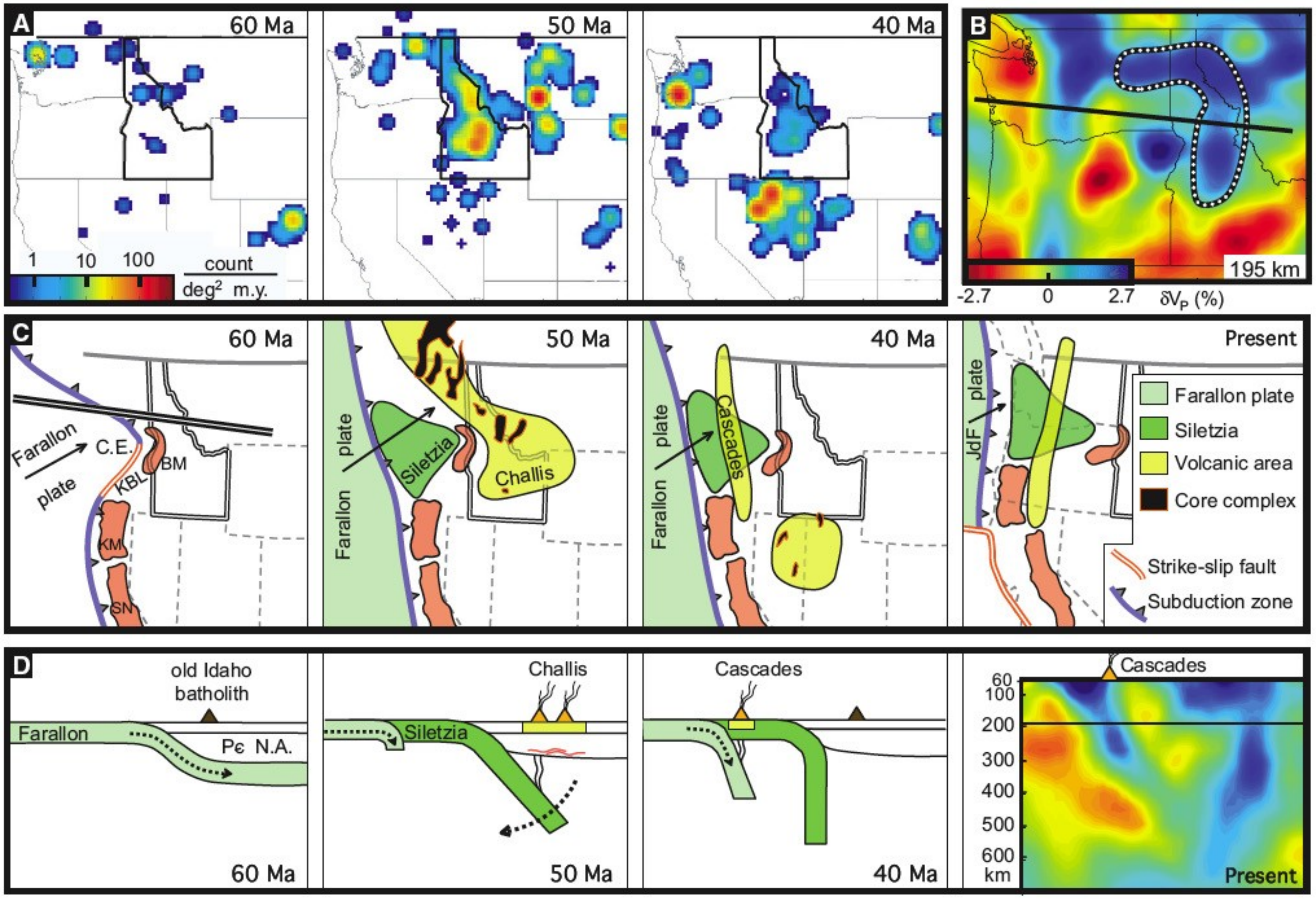

Figure 2. Maps and cross sections of northwestern United States at 60, 50, 40, and 0 Ma. Border of Idaho is highlighted. A: Maps showing density of reported dated igneous rocks from NAVDAT (North American volcanic and intrusive rock database; Walker et al., 2004). Data are binned in time and space (age data distributed equally over reported range, and age uncertainty >10 m.y. rejected). Results are smoothed over 50 km in space and 1 m.y. in time. Large dynamic range requires log scale and indicates variations between lulls and flare-ups. B: P-wave tomography, emphasizing correlation between imaged curtain and Challis magmatism. Dotted line—Siletzia curtain outline. Dark line—location of cross-section A–A′. C: Maps illustrating regional tectonic and magmatic evolution, modified after Dickinson (2006). Intact and coherent units defined by presence of Mesozoic to Cretaceous plutons and associated arc-related rocks are shown in pink; Klamath Mountains (KM), Blue Mountains (BM), and Sierra Nevada (SN). Prior to accretion, 60 Ma, Klamath–Blue Mountains lineament (KBL) is shown as transform boundary (Riddihough et al., 1986). At 60 Ma Farallon plate subducted to northeast in Columbia Embayment (C.E.). Siletzia accreted and subduction stepped west ca. 55–53 Ma, and by 50 Ma Challis magmatism was strong (JdF—Juan de Fuca). D: Cross sections (along B–B′ shown in C, left panel) show our interpretation of subduction history. At 60 Ma, Farallon slab subducts flat against Precambrian (Pc) North America (N.A.). Then, shortly after Siletzia accretion (50 Ma), Cascadia subduction initiates and abandoned, previously flat Farallon slab rolls back, exposing basal North America and Farallon crust to inflowing asthenosphere, causing melting. Event is over by 40 Ma, and little has changed to present, represented by tomography cross section, A–A′.

Schamdt and Humphreys 2011

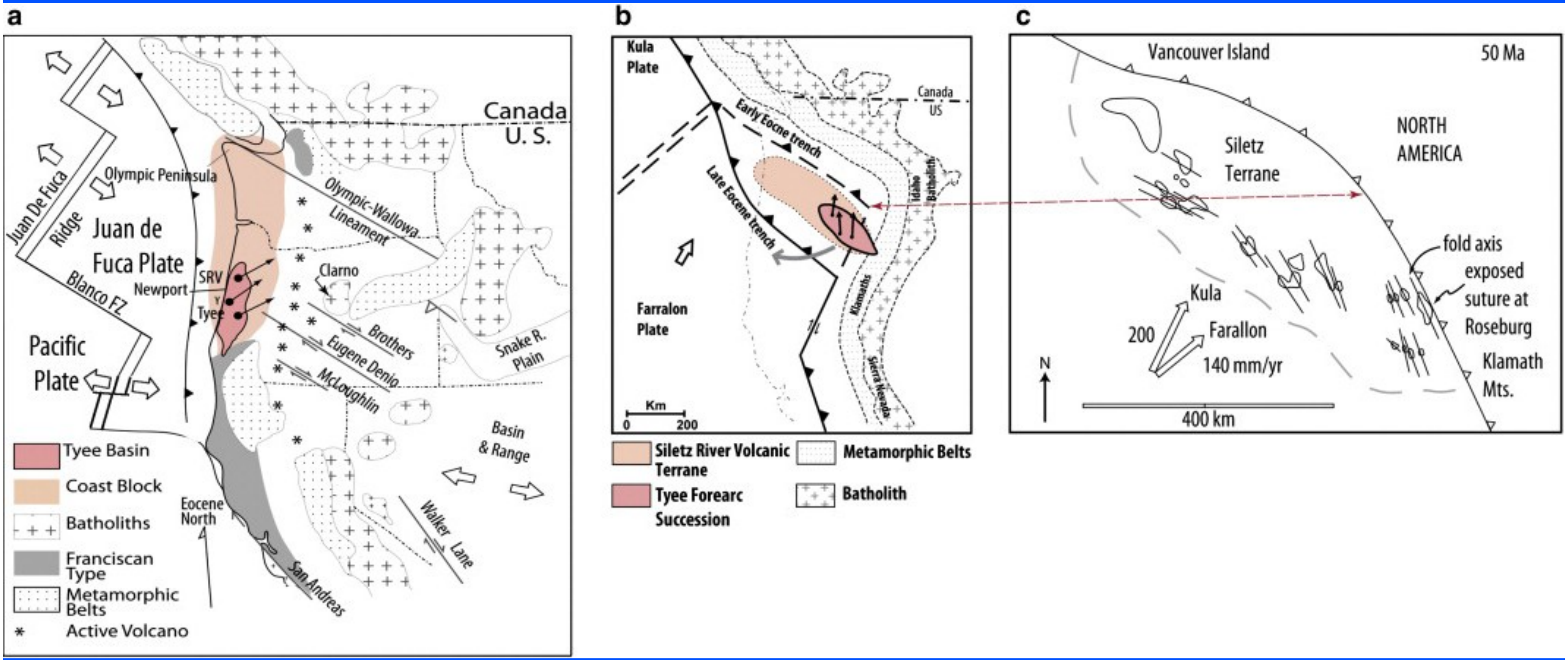

Fig. 3 Some important tectonic elements of the present-day western North America and a model for accretion and post-Early Eocene rotation of Siletz River Volcanics (SRV).

Santra et al 2013 Global and Planetary Change, Volume 103, 2013, 207 - 231